5-15-1993

Photoelectric and CCD Photometry of E and S0 Galaxies

M. Colless
Institute of Astronomy

D. Burstein
Arizona State University

G. Wegner
Dartmouth College

R. P. Saglia
Heidelberg-Königstuhl State Observatory

Mon. Not. R. Astron. Soc. **262,** 475–490 (1993)

Photoelectric and CCD photometry of E and S0 galaxies

Matthew Colless,[1]★ D. Burstein,[2] G. Wegner,[3] R. P. Saglia,[4] R. McMahan,[5] R. L. Davies,[6] E. Bertschinger[7] and G. Baggley[6]

[1]*Institute of Astronomy, Madingley Road, Cambridge CB3 0HA*
[2]*Department of Physics and Astronomy, Arizona State University, Tempe, AZ 85287-1504, USA*
[3]*Department of Physics and Astronomy, Dartmouth College, Wilder Laboratory, Hanover, NH 03755, USA*
[4]*Landessternwarte Heidelberg-Königstuhl, Königstuhl, D-6900 Heidelberg 1, Germany*
[5]*Department of Physics and Astronomy, University of North Carolina, CB # 3255 Phillips Hall, Chapel Hill, NC 27599, USA*
[6]*Department of Astrophysics, Keble Road, Oxford OX1 3RH*
[7]*Department of Physics, Massachusetts Institute of Technology, Cambridge, MA 02139, USA*

Accepted 1992 November 10. Received 1992 November 4; in original form 1992 September 10

ABSTRACT

We present *BR* photoelectric photometry for 352 E and S0 galaxies that are part of a large survey of the properties and peculiar motions of galaxies in distant clusters. Repeat measurements show our internal errors to be 2–3 per cent in B and R and 1–2 per cent in $B-R$. Comparisons of *BR* and *BVR* reductions for 10 galaxies also observed in V show small systematic errors due to differences between the spectral energy distributions of stars and galaxies. External comparisons with $B-V$ colours in the literature confirm that these colours are good to 1 per cent. We also describe R-band CCD observations for 95 of the galaxies and place these on a *BR* photometric system for photoelectric and CCD photometry, with a common zero-point good to better than 1 per cent. We find the rms precision of both our photoelectric and CCD R magnitudes to be 2–3 per cent for galaxies as faint as $R \approx 15$. Errors in galaxy magnitudes of this order introduce errors of $\lesssim 2$ per cent into D_n–σ distance estimates, corresponding to errors in peculiar velocities for single galaxies of $\lesssim 200$ km s^{-1} at a distance of 10 000 km s^{-1}.

Key words: galaxies: distances and redshifts – galaxies: elliptical and lenticular, cD – galaxies: photometry.

1 INTRODUCTION

Over the past decade, CCD photometry has replaced photoelectric photometry as the method of choice for absolute photometry of galaxies. This preference is due to the imaging capability, high quantum efficiency and ready availability of CCDs. In 1986 we began a combined photometric and spectroscopic study of more than 500 E and S0 galaxies in distant clusters, with the dual scientific goals of understanding the physical properties of these galaxies and using these same properties to measure the distances and peculiar velocities of the clusters. At the outset of this project, we realized that most of the photometry could best and most easily be carried out using CCDs. However, we decided to obtain both CCD *and* photoelectric photometry for as many of the galaxies in our survey as possible. This decision was based partly on the critical need for accurate photometric zero-points in order for our programme to attain its scientific goals. As pointed out by Dressler et al. (1987), errors in the photometric zero-points enter linearly into distance estimates for galaxies. Using the D_n–σ relation as defined by Dressler et al. to determine distances, a zero-point error of 0.01 mag (or 0.92 per cent) corresponds to an error in D_n of approximately 0.6 per cent. Thus zero-point errors of less than 0.03 mag are required to achieve distances accurate to better than 2 per cent (i.e. <200 km s^{-1} at a distance of 10 000 km s^{-1}). The second reason for our decision was that it was highly desirable that the present survey be reconcilable with the photoelectric data assembled in previous studies, especially the extensive '7 Samurai' (Faber et al. 1989).

Relatively little information exists in the literature on the degree of agreement between the zero-points and scales of CCD-calibrated and photoelectric-calibrated photometry of galaxies. Jørgensen, Franx & Kjærgaard (1992) have compared CCD and photoelectric measurements taken in the B band and have obtained results consistent with known observational errors of 1–2 per cent. Very little information exists concerning comparisons of galaxy observations in R, since relatively few photoelectric observations of galaxies have been made in this passband.

★Present address: Mt Stromlo Observatory, Australian National University, Canberra, A.C.T., Australia.

Our goal was to obtain CCD-calibrated R-passband photometry of our entire galaxy sample, and a separate photoelectric calibration in R for at least half of these galaxies. The photoelectric data would also yield $B-R$ colours. Only in this manner could we be sure that (i) our data could be reliably placed on the existing photoelectric-based photometric system for galaxies, (ii) that the true extent of zero-point differences between CCD and photoelectric systems would be known, and (iii) that all of our data would be on an internally self-consistent system.

These goals for the photoelectric data have been achieved, and in this paper we present the results of all the photoelectric photometry that was carried out for this survey. We also now have sufficient overlap between the CCD and photoelectric photometry to permit a detailed comparison of the R magnitudes obtained from these two methods. We emphasize the accuracy of the magnitudes, especially in the R passband, as it is the error in magnitude that directly affects the accuracy of distance measurements. Section 2 presents the photoelectric photometry for a total of 344 programme galaxies and a further eight standard galaxies. The accuracy of these magnitudes is evaluated primarily by internal comparisons, although comparisons are also made, where possible, with $B-V$ colours from the literature. Our methodology for obtaining aperture magnitudes from CCD images is described in Section 3. The CCD and photoelectric magnitudes are compared in Section 4, and our results are summarized in Section 5.

2 PHOTOELECTRIC PHOTOMETRY

2.1 Methods

The scientific goal of our photoelectric observations was to obtain galaxy B and R magnitudes that were accurate to 0.03 mag or better. The choice of these passbands was dictated in part by the use of the R passband in the CCD observations, and in part by the desire to be able eventually to tie these data directly to the B-passband measurements of Burstein et al. (1987).

All photoelectric observations for this programme were made with the 1.3-m Kitt Peak National Observatory (KPNO) telescope, equipped with the Mark III photometer. The Landolt (1983) list of *UBVRI* standard stars was used as the source for standardization of the photometry. A log of the observations is given in Table 1, listing the night of observation (local time), the photomultiplier (identified by both photocathode type and KPNO Cold Box designation) and filter system, the photometric quality, Q, of the night (defined below), the number of observations of Landolt standard stars that were made, the number of individual Landolt standard stars observed, the number of standard galaxies (defined below) observed, and the number of programme galaxies observed.

The programme galaxies were observed in the B and R filters. Two important sources of error in the determination of galaxy magnitudes are photon noise and zero-point errors in the transformation of magnitudes to a standard system. Adequate integration time can solve the first problem. The second problem requires that a set of well-observed bright galaxies, not in our programme, be established as 'standard' galaxies to help zero our magnitudes to an internally consistent *BR* system.

The standard galaxies and the standard stars were observed in *BVR*, as the addition of the V filter took little extra time. Separate integrations were taken every 10 s for the galaxies, and every 5 s for the standard stars. Sets of 10-s integrations were arranged so that no more than 4 min separated any galaxy observation from a sky observation in the same filter. No attempt was made to compensate for faint stars within the photoelectric apertures, although the smaller aperture sizes were used to avoid stars where possible. The photoelectric magnitudes therefore include everything on the sky within the aperture when it is centred on the galaxy.

The chief problem in obtaining accurate galaxy magnitudes is the same as for stellar magnitudes, namely monitoring of nightly extinction. To overcome this, standard stars were chosen with a range of $B-R$ colours that bracketed the galaxy colours. Nightly observations tried to balance a wide sample of individual stars with multiple observations of several stars over a range in airmass. Many different stars were observed within a given observing run, to average over the known errors in the standard star magnitudes (sometimes $\gtrsim 0.01$ mag).

On any given night, all galaxy observations were sandwiched between standard star observations, which were obtained approximately on an hourly basis. Observations were greatly enhanced by the fast slewing ability of the 1.3-m telescope and the on-line data reduction capability of the Mark III photometer. Standard star observations took an average of 2.7 min between any two points in the sky. We typically observed six standard stars at all airmasses, east and west, every hour, together with more stars at the beginning and end of the night. As is evident in Table 1, we observed between five and seven stars an hour, depending on the length of the night.

The on-line data reduction provided by the Mark III photometer, combined with our observing strategy, per-

Table 1. Log of photoelectric observations.

Date	Instrumental setup (MkIII photometer +)	Q	# std obsns	# std stars	# std gals	# gals
88.05.07	#27 S-20 + 'K' UBVR	B	58	28	2	18
88.05.08	#27 S-20 + 'K' UBVR	B	57	23	2	18
88.05.09	#51 GaAs + 'J' UBVRI	A	50	18	1	26
88.05.10	#51 GaAs + 'J' UBVRI	A	50	22	2	22
90.06.19	#54 S-20 + 'K' UBVR	B	31	21	1	7
90.06.20	#54 S-20 + 'K' UBVR	B	36	21	1	16
90.06.21	#54 S-20 + 'K' UBVR	B	29	21	1	12
90.08.20	#54 S-20 + 'K' UBVR	A	62	21	2	15
90.08.21	#54 S-20 + 'K' UBVR	A	59	25	0	15
90.08.22	#54 S-20 + 'K' UBVR	A	55	22	2	19
90.08.23	#54 S-20 + 'K' UBVR	A	57	29	1	19
91.05.15	#54 S-20 + 'K' UBVR	A	22	15	0	7
91.05.16	#54 S-20 + 'K' UBVR	A	39	20	2	15
91.05.17	#54 S-20 + 'K' UBVR	A	37	21	2	16
91.05.18	#54 S-20 + 'K' UBVR	A	36	18	0	9
91.07.09	#54 S-20 + 'K' UBVR	A	49	22	1	12
91.07.10	#54 S-20 + 'K' UBVR	A	41	23	2	16
91.07.11	#54 S-20 + 'K' UBVR	A	20	12	1	8
91.07.12	#54 S-20 + 'K' UBVR	B	20	12	1	6
91.10.03	#54 S-20 + 'K' UBVR	A	23	17	0	6
91.10.04	#54 S-20 + 'K' UBVR	A	36	21	1	15
91.10.05	#54 S-20 + 'K' UBVR	A	33	21	2	22
91.10.10	#54 S-20 + 'K' UBVR	A	56	28	2	15
91.10.12	#54 S-20 + 'K' UBVR	A	30	13	0	9
91.10.13	#54 S-20 + 'K' UBVR	A	45	20	0	22
91.10.14	#54 S-20 + 'K' UBVR	A	51	25	2	24
		Total:	1082	539	31	389

mitted us to monitor extinction variations during each night on an hourly basis. On most nights we found that the Kitt Peak sky experienced temporal variations of 1–3 per cent in the zero-point of extinction that were relatively grey and adiabatic, in that they were consistent over the whole sky at all airmasses and in all filters. On several nights, these adiabatic changes in transparency were confirmed by comparing the 1.3-m measures to those being taken by other observers on the 0.9-m KPNO telescope. For each run, the uniformity of the photomultiplier was established by scanning a bright star across the field of view.

On 1988 May 8 we sadly witnessed the demise of the very sensitive Cold Box # 27 S-20 photomultiplier, which lost its stability during this night. This was unfortunate, as the substitute S-20 cold box we used for most of the remainder of the survey (# 54) was 1 mag less sensitive than Box # 27 in B, and 1.7 mag less sensitive in R. The loss of Cold Box # 27 cost us the ability to obtain two aperture observations per galaxy, as originally planned, so that most galaxies were observed through one aperture only.

Of the first 59 nights allotted to this programme, only 11 nights (19 per cent) were usable; of the last 20.5 nights, 14.5 (71 per cent) were usable. Thus, while our overall success rate is somewhat better than average for KPNO (32 per cent), it came at the expense of many discouraging nights at the beginning of the programme.

The extinction and transformation coefficients for each night were derived in a graphical, iterative manner. A graphical manner was chosen for the reduction, as it is often found that 'wild' observations bias the result if a blind multiparameter least-squares fit is made. These wild observations result from a number of factors, including pointing at the wrong star, loss of aperture centring, poor focus, variable standard stars (several were found), or poor standard star magnitudes. All nights within each run were reduced both separately and as part of the run, to improve the precision of the transformation to the standard system. Differential changes in extinction from night to night were absorbed into the temporal terms for a given night. The transformation coefficient for B magnitudes was the same for all runs with Cold Box # 54 (the only photomultiplier used on more than one run), while that for the $B-R$ term differed by 0.02 mag between the 1990 and 1991 runs.

For 19.5 nights the temporal changes in extinction during a night were less than 0.030 mag, and the resulting *total* dispersions of B, V and R magnitudes for the standard stars were less than 0.015 mag. These nights are given a quality code of 'A' (see Table 1). On six nights the stability of the sky (or, on 1988 May 8, the photometer), once temporal changes were removed, was 0.015–0.030 mag in all filters. These nights are given a quality code of 'B'. Observations were also made on seven other nights, but during reduction it was found that the standard star observations had a scatter of >0.03 mag, even after removing temporal changes. These nights we classify as quality 'C'. As discussed in the following section, comparison of galaxy observations taken on C nights with those taken on A or B nights show the C-night observations to be of inferior quality, so they are only used for comparison purposes in this paper.

Due to the fact that the programme galaxies were only observed in BR, while the standard stars and standard galaxies were observed in BVR, the standard stars were reduced in both BR and BVR. Galaxy magnitudes were then predicted from the BR transformations obtained in each reduction. The reliability of this transformation is evaluated below by both internal and external comparisons.

All the photoelectric photometry taken on A- or B-quality nights is presented in Tables 2 and 3. In each table are given the ID number of the galaxy used in these studies, the galaxy's name and (in Table 2) position, the date, time and airmass of the observation, the diameter of the photometric aperture used (in arcsec), the quality of the observation (A or B), the measured B and R magnitudes and $B-R$ colour of the galaxy (Table 2), or BVR, $B-V$ and $B-R$ (Table 3).

The positions for all programme galaxies were determined by one of us (DB) using the Guide Star Astrometric Support System (GASP) of the Space Telescope Science Institute (STScI). These positions were originally calculated in J2000 coordinates and then precessed to B1950 coordinates. The positions are quoted to ~1-arcsec precision, which is about the expected uncertainty due to centring errors (and which dominates the errors of ~0.5 arcsec from the GASP astrometry). Positions for non-programme galaxies were obtained from either the RC2 (de Vaucouleurs, de Vaucouleurs & Corwin 1978) or, for the Coma cluster galaxies, Faber et al. (1989).

For most galaxies, the B and R magnitudes are formally determined to better than 1 per cent in terms of photon-statistical errors. These magnitudes are corrected to zero airmass, but have no corrections applied for either Galactic extinction or the K-correction. Table 2 lists a total of 397 BR photoelectric observations of 344 programme galaxies (including two galaxies in the Coma cluster) and 38 observations of eight standard galaxies. There are two or more BR photoelectric observations for 43 of the programme galaxies and for six of the standard galaxies. Table 3 gives BVR data from 31 observations of eight standard galaxies and two observations of two programme galaxies.

2.2 Internal comparisons

Two types of internal comparison can be made within the photoelectric data set. The first is a straightforward comparison of observations of the same galaxy made with the same aperture on different nights. The second is a comparison of the photometry when it is reduced in two different ways. One reduction procedure is used for all galaxies, both programme and standard, and uses the results of the BR reduction of the standard stars. The other reduction procedure uses the results of the BVR reduction of the standard stars to predict BR magnitudes for those few galaxies (mostly standard galaxies) with BVR observations. This second type of comparison cross-checks the degree to which the standard stars can consistently transform the galaxy colours. This is always of concern, given that the spectral energy distributions of galaxies are not the same as those of stars with the same colours.

2.2.1 *Repeat photoelectric observations*

Nights of quality A and B were stable to 1–3 per cent, while nights of quality C were much less stable. Of the 435 independent observations of programme and standard galaxies which were of quality A or B, 98 were duplicated with the same galaxy and the same aperture, but on *different* nights of quality A or B. There were also 96 duplicate observations that combined nights of quality C with other nights. Included

Table 2. *BR* photoelectric data.

ID#	Name	R.A. (1950)	Dec.	Date	UT	Air	D (″)	Q	B	R	B−R
1	A76 A	00 36 51.2	+06 27 35	91.10.05	05:46	1.175	29.9	A	15.225	13.379	1.846
2	A76 B	00 37 53.0	+06 26 43	91.10.05	05:57	1.159	29.9	A	15.901	14.206	1.696
4	A76 D	00 37 55.5	+06 38 35	91.10.14	06:11	1.108	29.9	A	15.778	14.023	1.755
5	A76 E	00 36 19.7	+06 47 17	91.10.14	06:23	1.103	19.2	A	15.972	14.117	1.855
6	A76 F	00 36 29.4	+07 13 05	91.10.14	06:39	1.101	19.2	A	16.035	14.199	1.835
10	J29 C	00 40 22.9	−09 30 16	91.10.04	06:56	1.331	29.9	A	16.980	15.153	1.827
13	A119 A	00 53 52.3	−01 31 59	90.08.22	09:33	1.214	29.9	A	15.359	13.631	1.728
14	A119 B	00 53 42.7	−01 31 33	90.08.22	09:45	1.205	29.9	A	15.380	13.595	1.785
15	A119 C	00 55 01.6	−01 39 40	90.08.22	09:59	1.199	29.9	A	15.526	13.789	1.737
17	A119 E	00 53 29.3	−01 36 17	90.08.22	10:16	1.197	29.9	A	15.934	14.253	1.681
21	A119 I	00 54 54.3	−00 44 31	91.10.05	06:09	1.252	29.9	A	16.056	14.187	1.869
24	A119 2	00 52 48.1	−01 37 24	91.10.05	06:27	1.228	29.9	A	16.619	15.415	1.205
25	J3 A	00 59 22.8	+26 40 59	91.07.10	09:56	1.335	29.9	A	15.614	13.789	1.825
26	J3 B	00 56 05.3	+26 42 29	91.07.10	10:14	1.254	29.9	A	16.209	14.431	1.779
27	J3 C	00 56 42.2	+26 47 23	91.07.10	10:30	1.202	29.9	A	15.662	14.011	1.651
31	J4 A	00 56 13.6	+12 42 11	91.10.03	07:59	1.063	29.9	A	15.168	13.380	1.788
32	J4 B	00 56 58.5	+12 43 00	91.10.03	08:10	1.069	29.9	A	16.010	14.303	1.708
38	A150 C	01 05 37.6	+01 55 38	91.10.04	07:28	1.153	29.9	A	15.831	14.064	1.767
39	A150 D	01 05 40.2	+01 54 36	91.10.04	08:09	1.164	29.9	A	16.387	14.756	1.631
40	A150 E	01 06 08.9	+01 55 32	91.10.04	08:29	1.186	29.9	A	16.730	15.023	1.708
43	A160 A	01 09 47.9	+15 29 06	90.08.20	10:11	1.047	29.9	A	15.685	13.993	1.692
44	A160 B	01 09 44.1	+15 27 39	90.08.23	09:26	1.067	19.2	A	17.180	15.330	1.850
45	A160 C	01 07 49.5	+15 55 29	90.08.22	10:54	1.047	29.9	A	16.148	14.281	1.867
46	A160 D	01 09 39.0	+16 03 39	90.08.23	09:07	1.091	29.9	A	16.563	14.694	1.869
47	A160 E	01 10 36.3	+15 15 05	90.08.22	11:13	1.059	29.9	A	15.732	13.989	1.743
47	A160 E	01 10 36.3	+15 15 05	90.08.23	10:44	1.046	29.9	A	15.712	13.983	1.729
50	A160 H	01 11 08.2	+15 14 36	90.08.23	10:13	1.044	19.2	A	16.812	15.119	1.693
51	A160 I	01 08 45.6	+15 18 26	90.08.23	10:28	1.043	19.2	A	16.722	14.809	1.913
52	A160 J	01 11 34.8	+15 38 02	90.08.20	10:24	1.042	29.9	A	15.653	14.068	1.585
56	A168 A	01 10 26.5	−00 31 05	91.10.12	08:58	1.328	29.9	A	14.319	12.708	1.610
58	A168 C	01 11 47.8	−00 05 05	91.10.13	05:36	1.271	19.2	A	16.381	14.644	1.737
59	A168 D	01 12 23.8	+00 09 58	91.10.12	08:42	1.276	29.9	A	15.594	13.801	1.793
60	A168 E	01 12 20.6	+00 02 19	91.10.12	09:09	1.356	29.9	A	16.453	14.623	1.830
62	A168 G	01 13 39.2	−00 22 20	91.10.13	05:52	1.247	19.2	A	16.605	14.849	1.757
70	J30 B	01 18 27.4	−14 05 49	91.10.13	06:50	1.442	19.2	A	16.915	15.167	1.748
73	J30 E	01 17 52.5	−14 09 06	91.10.10	07:30	1.437	19.2	A	16.680	15.010	1.670
73	J30 E	01 17 52.5	−14 09 06	91.10.13	07:06	1.436	19.2	A	16.707	15.042	1.665
79	A193 B	01 22 34.7	+08 23 44	91.10.10	05:52	1.177	29.9	A	16.776	14.966	1.810
81	A193 D	01 22 01.4	+08 14 58	91.10.10	06:13	1.145	29.9	A	15.988	14.238	1.750
85	J32 B	01 34 54.1	−09 25 23	91.10.03	08:45	1.343	29.9	A	15.686	14.023	1.662
96	A260 A	01 47 49.4	+32 50 04	90.08.23	10:58	1.001	29.9	A	15.116	13.340	1.776
98	A260 C	01 48 30.0	+32 47 02	90.08.23	11:09	1.000	29.9	A	15.472	13.712	1.760
100	A260 E	01 46 19.6	+32 50 51	91.10.10	06:31	1.046	29.9	A	15.755	14.020	1.734
101	A260 F	01 47 21.7	+33 14 52	91.10.14	07:37	1.000	29.9	A	15.670	13.935	1.736
102	A260 G	01 48 51.4	+33 17 26	91.10.14	07:48	1.001	19.2	A	16.035	14.273	1.762
105	A262 A	01 49 50.0	+35 54 21	91.10.05	07:45	1.010	29.9	A	14.652	12.981	1.671
106	A262 B	01 47 55.1	+36 01 42	91.10.05	08:02	1.005	29.9	A	13.367	11.858	1.509
107	A262 C	01 47 37.1	+36 07 24	91.10.05	08:13	1.003	29.9	A	14.240	12.537	1.702
108	A262 D	01 46 48.2	+35 32 15	91.10.05	08:19	1.002	29.9	A	14.209	12.472	1.737
110	A262 F	01 50 11.5	+36 34 25	91.10.14	08:03	1.006	19.2	A	14.995	13.178	1.817
113	A262 I	01 49 43.3	+35 55 30	91.10.05	08:25	1.003	29.9	A	15.084	13.318	1.766
115	J7 A	02 22 35.1	+36 44 21	91.10.03	09:02	1.004	29.9	A	15.350	13.586	1.764
117	J7 C	02 20 53.0	+36 50 11	91.10.04	08:55	1.004	29.9	A	15.683	14.014	1.669
117	J7 C	02 20 53.0	+36 50 11	91.10.04	09:29	1.011	29.9	A	15.630	13.939	1.691
118	J7 D	02 23 24.2	+36 48 56	91.10.04	09:40	1.018	29.9	A	16.399	14.667	1.732
119	J7 E	02 23 11.0	+37 04 02	91.10.04	10:02	1.038	29.9	A	15.967	14.245	1.722
122	J8 A	02 27 25.5	+22 55 54	91.10.10	08:31	1.012	29.9	A	15.544	13.741	1.803
127	J8 F	02 26 44.3	+22 43 14	91.10.10	08:42	1.014	29.9	A	16.087	14.184	1.903

Table 2 – *continued*

ID#	Name	R.A. (1950)	Dec.	Date	UT	Air	D (″)	Q	B	R	B−R
128	J8 G	02 27 40.3	+22 43 39	91.10.10	08:59	1.018	19.2	A	16.059	14.256	1.804
128	J8 G	02 27 40.3	+22 43 39	91.10.13	06:08	1.171	19.2	A	16.072	14.225	1.847
130	J8 I	02 26 23.3	+22 44 37	91.10.10	09:15	1.027	19.2	A	16.639	14.709	1.931
130	J8 I	02 26 23.3	+22 44 37	91.10.13	06:19	1.139	19.2	A	16.615	14.670	1.945
132	J8 K	02 24 42.6	+22 50 10	91.10.03	09:26	1.017	29.9	A	16.236	14.378	1.859
137	A376 C	02 42 37.4	+36 38 40	91.10.04	10:55	1.091	29.9	A	16.663	14.904	1.759
146	J9 E	02 48 54.9	+46 42 30	91.10.05	08:57	1.038	29.9	A	16.057	14.143	1.914
151	A397 A	02 53 46.1	+15 42 33	91.10.13	08:19	1.047	19.2	A	16.273	14.414	1.859
153	A397 C	02 53 41.0	+15 48 25	91.10.13	08:34	1.042	19.2	A	16.275	14.467	1.808
154	A397 D	02 54 17.7	+15 46 57	91.10.13	09:03	1.042	19.2	A	16.536	14.705	1.831
155	A397 E	02 53 45.6	+15 48 11	91.10.05	09:08	1.042	29.9	A	16.575	14.793	1.782
157	A397 G	02 54 50.6	+15 52 04	91.10.13	08:52	1.040	19.2	A	16.096	14.239	1.857
158	A397 H	02 55 10.5	+15 54 20	91.10.13	07:33	1.089	19.2	A	16.851	14.942	1.909
160	A400 A	02 54 55.2	+05 46 36	91.10.05	09:23	1.113	29.9	A	15.667	13.798	1.869
162	A400 C	02 52 36.3	+05 58 31	91.10.05	09:33	1.115	29.9	A	16.209	14.199	2.010
163	A400 D	02 55 35.7	+05 46 20	91.10.12	09:46	1.142	29.9	A	16.274	14.374	1.899
164	A400 E	02 55 42.4	+05 53 44	91.10.12	10:02	1.157	29.9	A	15.724	13.866	1.858
166	A400 G	02 56 15.6	+05 55 02	91.10.12	10:14	1.184	29.9	A	16.383	14.637	1.747
169	A400 J	02 55 45.6	+06 23 33	91.10.12	10:36	1.214	29.9	A	15.346	13.422	1.924
174	J28 A	03 05 49.9	−04 19 46	91.10.05	10:15	1.254	29.9	A	14.736	13.077	1.659
175	J28 B	03 05 14.6	−04 30 38	91.10.05	10:21	1.266	29.9	A	15.538	13.810	1.729
176	J28 C	03 05 33.3	−04 35 27	91.10.05	10:32	1.278	29.9	A	15.225	13.533	1.692
177	A419 A	03 06 03.7	−23 52 56	91.10.03	10:21	1.816	29.9	A	16.121	14.336	1.785
182	A419 F	03 06 09.3	−23 50 14	91.10.14	08:33	1.777	19.2	A	17.016	15.203	1.814
184	A419 H	03 06 03.9	−23 45 17	91.10.14	08:54	1.764	19.2	A	16.762	14.930	1.832
185	A419 I	03 06 36.1	−23 37 32	91.10.14	09:11	1.768	19.2	A	17.158	15.361	1.797
189	A496 A	04 31 18.7	−13 21 57	91.10.10	09:58	1.444	29.9	A	15.145	13.305	1.840
190	A496 B	04 31 51.5	−13 28 24	91.10.10	10:10	1.433	19.2	A	16.307	14.494	1.814
190	A496 B	04 31 51.5	−13 28 24	91.10.14	09:55	1.434	19.2	A	16.292	14.465	1.827
192	A496 D	04 31 38.2	−13 33 58	91.10.14	10:05	1.429	19.2	A	16.341	14.536	1.805
193	A496 1	04 32 48.1	−13 29 47	91.10.10	10:43	1.424	19.2	A	16.724	14.844	1.881
193	A496 1	04 32 48.1	−13 29 47	91.10.14	10:16	1.423	19.2	A	16.723	14.818	1.905
195	A496 3	04 31 13.0	−13 16 35	91.10.14	10:31	1.419	19.2	A	16.407	14.646	1.761
196	J34 A	04 42 55.8	−15 57 40	91.10.10	11:21	1.505	29.9	A	14.950	13.155	1.795
197	J34 B	04 43 05.9	−15 52 55	91.10.13	09:42	1.536	29.9	A	15.953	14.231	1.723
198	J34 C	04 43 19.6	−16 06 43	91.10.05	10:45	1.505	29.9	A	16.045	14.346	1.699
199	J34 D	04 43 15.7	−16 09 43	91.10.13	10:15	1.500	19.2	A	16.455	14.799	1.656
200	J34 E	04 41 29.6	−15 54 34	91.10.13	10:55	1.495	19.2	A	16.323	14.591	1.731
201	J34 F	04 45 35.8	−15 36 46	91.10.13	09:59	1.505	29.9	A	15.359	13.607	1.752
206	J10 A	04 50 14.2	+01 10 37	91.10.12	11:48	1.201	29.9	A	15.147	13.361	1.786
208	J10 C	04 50 53.7	+01 12 03	91.10.05	11:01	1.166	29.9	A	16.357	14.742	1.615
209	P597-1 A	04 56 21.5	−00 33 51	91.10.12	11:08	1.186	29.9	A	14.569	12.781	1.788
210	P597-1 B	04 56 10.9	−00 33 12	91.10.13	11:12	1.189	29.9	A	15.318	13.560	1.758
211	P597-1 C	04 56 00.2	−00 37 43	91.10.13	11:22	1.197	19.2	A	15.632	13.858	1.774
215	J35 A	04 52 39.5	−18 11 42	91.10.13	11:50	1.632	29.9	A	14.978	13.265	1.713
216	J35 B	04 54 52.1	−18 21 46	91.10.13	11:34	1.603	29.9	A	15.754	14.018	1.736
251	A533-1 C	05 01 45.2	−23 35 09	91.10.14	11:15	1.776	29.9	A	15.638	13.947	1.691
255	A533-1 G	04 59 06.5	−24 00 53	91.10.14	10:59	1.784	29.9	A	15.734	14.075	1.659
266	A548-1 A	05 46 36.5	−25 29 35	91.10.14	11:32	1.854	29.9	A	15.252	13.602	1.650
273	A548-1 H	05 47 19.7	−25 21 39	91.10.14	11:48	1.851	29.9	A	15.275	13.659	1.616
302	J11 A	13 03 28.1	+53 49 52	88.05.10	04:30	1.086	29.9	A	15.472	13.870	1.601
303	J11 B	13 03 47.9	+53 55 35	88.05.08	04:09	1.106	29.9	B	15.468	13.881	1.587
303	J11 B	13 03 47.9	+53 55 35	88.05.07	04:05	1.113	60.2	B	14.699	12.942	1.757
304	J11 C	13 03 23.9	+53 57 08	88.05.07	04:14	1.105	39.5	B	15.099	13.453	1.646
304	J11 C	13 03 23.9	+53 57 08	88.05.08	04:17	1.097	39.5	B	15.090	13.470	1.620
304	J11 C	13 03 23.9	+53 57 08	88.05.09	04:48	1.082	39.5	A	15.096	13.489	1.607
304	J11 C	13 03 23.9	+53 57 08	88.05.10	04:38	1.084	39.5	A	15.070	13.458	1.612
305	J11 D	13 02 54.5	+53 55 17	88.05.09	04:55	1.079	39.5	A	15.386	13.822	1.565

Table 2 – *continued*

ID#	Name	R.A. (1950)	Dec.	Date	UT	Air	D (″)	Q	B	R	B–R
306	J11 E	13 03 17.4	+53 51 32	91.05.17	04:41	1.077	29.9	A	15.547	14.177	1.371
307	J11 F	13 05 14.1	+53 51 11	88.05.09	04:41	1.084	39.5	A	15.470	13.899	1.570
310	J12 A	13 41 08.0	+30 19 13	88.05.07	04:46	1.038	29.9	B	15.388	13.755	1.633
310	J12 A	13 41 08.0	+30 19 13	90.06.20	05:18	1.128	39.5	B	15.255	13.632	1.623
311	J12 B	13 40 38.4	+30 07 11	91.05.16	04:15	1.039	29.9	A	15.376	13.718	1.658
312	J12 C	13 40 31.4	+29 57 24	91.05.16	04:28	1.024	29.9	A	16.053	14.429	1.624
313	J12 D	13 41 57.2	+30 03 16	91.05.16	04:44	1.014	29.9	A	16.329	14.590	1.740
314	J12 E	13 40 06.1	+30 05 57	91.05.16	05:02	1.004	29.9	A	15.746	14.141	1.605
315	J12 F	13 40 06.3	+30 04 34	88.05.07	04:33	1.056	29.9	B	15.660	13.947	1.713
318	J13 A	13 52 54.7	+25 17 45	88.05.07	05:55	1.010	39.5	B	14.783	13.148	1.635
318	J13 A	13 52 54.7	+25 17 45	88.05.07	05:50	1.012	60.2	B	14.568	12.977	1.591
319	J13 B	13 52 53.8	+25 15 56	88.05.07	06:02	1.008	39.5	B	15.254	13.762	1.493
321	J13 D	13 52 37.1	+25 22 02	91.05.17	05:20	1.008	29.9	A	15.638	13.866	1.772
322	J13 E	13 51 21.8	+25 19 28	88.05.07	06:09	1.007	39.5	B	15.591	13.879	1.712
323	J13 F	13 50 25.9	+25 17 08	88.05.07	06:17	1.007	39.5	B	15.349	13.831	1.519
324	J13 G	13 50 18.2	+24 59 40	88.05.07	06:25	1.009	39.5	B	14.843	13.255	1.588
325	J13 H	13 48 46.2	+25 20 24	88.05.07	06:33	1.011	39.5	B	14.837	13.249	1.588
327	J13 J	13 48 12.5	+25 13 13	88.05.07	06:45	1.016	39.5	B	15.389	13.904	1.485
328	J13 K	13 48 11.5	+25 12 35	91.07.10	04:37	1.232	29.9	A	15.710	14.007	1.703
329	J13 L	13 48 05.7	+25 09 21	91.07.10	04:53	1.289	29.9	A	16.652	14.930	1.722
330	J13 M	13 47 33.3	+25 26 17	88.05.07	06:53	1.021	39.5	B	15.474	14.069	1.406
331	J13 N	13 53 29.5	+25 02 57	91.07.10	05:09	1.334	29.9	A	16.572	14.924	1.648
333	J13 P	13 53 50.8	+25 26 21	91.05.17	06:03	1.013	29.9	A	16.090	14.465	1.625
336	J36 A	14 05 27.7	−08 50 06	88.05.07	07:17	1.360	29.9	B	15.031	13.376	1.655
339	J36 D	14 03 57.3	−08 59 29	88.05.07	07:26	1.384	39.5	B	15.494	13.920	1.574
343	J14 A	14 44 39.3	+13 52 35	88.05.08	04:36	1.264	39.5	B	15.198	13.593	1.605
343	J14 A	14 44 39.3	+13 52 35	88.05.09	05:28	1.130	39.5	A	15.172	13.567	1.605
344	J14 B	14 44 16.3	+13 53 05	88.05.08	04:48	1.232	29.9	B	15.780	14.128	1.652
344	J14 B	14 44 16.3	+13 53 05	88.05.09	05:34	1.110	39.5	A	15.646	14.028	1.618
345	J14 C	14 44 24.9	+13 54 12	91.05.17	06:20	1.053	29.9	A	16.746	15.265	1.481
352	J14-1 A	14 44 41.7	+11 48 08	88.05.08	05:27	1.154	39.5	B	14.757	13.120	1.636
352	J14-1 A	14 44 41.7	+11 48 08	88.05.09	05:55	1.104	39.5	A	14.720	13.097	1.623
353	J14-1 B	14 44 29.2	+11 50 05	91.05.17	06:44	1.069	29.9	A	15.466	13.864	1.602
354	J14-1 C	14 44 21.9	+11 46 43	88.05.08	05:35	1.139	29.9	B	15.575	13.898	1.677
354	J14-1 C	14 44 21.9	+11 46 43	88.05.09	06:02	1.096	39.5	A	15.398	13.746	1.652
355	J14-1 D	14 44 03.0	+11 42 58	88.05.08	05:42	1.128	29.9	B	15.253	13.683	1.571
355	J14-1 D	14 44 03.0	+11 42 58	88.05.09	06:10	1.088	39.5	A	15.115	13.640	1.475
356	J14-1 E	14 44 41.9	+11 12 29	88.05.08	05:49	1.122	29.9	B	15.887	14.276	1.611
357	J14-1 F	14 46 42.6	+11 11 11	91.07.11	04:44	1.197	19.2	A	15.987	14.396	1.590
362	A1983-1 A	14 52 03.3	+16 33 27	88.05.08	05:57	1.084	39.5	B	15.058	13.326	1.732
362	A1983-1 A	14 52 03.3	+16 33 27	88.05.09	06:38	1.044	39.5	A	15.003	13.314	1.689
363	A1983-1 B	14 50 35.3	+16 54 23	88.05.08	06:06	1.067	29.9	B	16.202	14.594	1.609
363	A1983-1 B	14 50 35.3	+16 54 23	88.05.09	06:50	1.038	39.5	A	15.964	14.308	1.657
364	A1983-1 C	14 50 36.9	+16 55 53	91.05.16	06:03	1.045	29.9	A	16.233	14.525	1.709
365	A1983-1 D	14 50 23.5	+17 06 27	88.05.08	06:19	1.056	29.9	B	15.766	14.021	1.746
365	A1983-1 D	14 50 23.5	+17 06 27	88.05.09	07:02	1.035	39.5	A	15.577	13.931	1.646
366	A1983-1 E	14 50 03.2	+17 19 32	91.05.16	06:20	1.036	29.9	A	15.911	14.217	1.693
367	A1983-1 F	14 47 39.0	+17 00 58	91.05.16	06:42	1.037	29.9	A	16.748	15.137	1.611
372	A1983 A	14 52 13.3	+18 50 41	91.05.16	07:30	1.052	29.9	A	15.968	14.176	1.792
375	A1983 D	14 48 56.0	+18 57 45	91.07.11	05:00	1.178	29.9	A	16.336	14.616	1.720
376	A1983 E	14 48 59.3	+18 53 31	88.05.10	05:21	1.101	39.5	A	15.464	13.801	1.663
377	A1983 F	14 51 21.2	+18 16 23	91.07.11	05:21	1.230	29.9	A	16.460	14.671	1.789
383	J16 A	15 16 31.9	+04 42 05	88.05.08	06:59	1.139	29.9	B	15.239	13.538	1.701
383	J16 A	15 16 31.9	+04 42 05	88.05.09	07:16	1.128	39.5	A	14.996	13.324	1.672
383	J16 A	15 16 31.9	+04 42 05	88.05.08	07:04	1.136	60.2	B	14.616	13.032	1.584
384	J16 B	15 16 33.7	+04 30 51	88.05.08	07:12	1.134	29.9	B	15.445	13.732	1.714
384	J16 B	15 16 33.7	+04 30 51	88.05.09	07:26	1.128	29.9	A	15.440	13.692	1.748
385	J16 C	15 15 58.3	+04 51 24	90.06.19	05:14	1.136	29.9	B	16.205	14.630	1.575

Table 2 – *continued*

ID#	Name	R.A. (1950)	Dec.	Date	UT	Air	D (″)	Q	B	R	B–R
386	J16 D	15 18 52.8	+04 31 13	88.05.08	07:20	1.129	29.9	B	15.960	14.162	1.798
386	J16 D	15 18 52.8	+04 31 13	88.05.09	07:35	1.128	39.5	A	15.777	13.939	1.839
387	J16 E	15 14 53.0	+04 23 45	91.05.16	07:49	1.155	29.9	A	15.788	14.112	1.676
388	J16 F	15 16 55.1	+04 45 36	91.05.16	08:07	1.172	19.2	A	16.470	14.754	1.716
396	J16-W B	15 09 01.7	+04 42 18	91.07.10	05:58	1.452	29.9	A	15.594	13.929	1.665
398	J16-W D	15 10 23.2	+04 42 00	88.05.08	07:43	1.128	29.9	B	15.517	13.850	1.667
399	J16-W E	15 10 40.7	+04 40 05	88.05.08	07:54	1.134	29.9	B	15.787	14.172	1.615
406	A2063-S A	15 19 29.3	+08 36 06	91.05.17	07:20	1.093	29.9	A	15.192	13.507	1.686
408	A2063-S C	15 19 10.2	+07 53 51	91.05.17	07:33	1.107	29.9	A	16.115	14.374	1.741
410	A2040 B	15 10 20.4	+07 37 14	91.07.11	05:59	1.423	29.9	A	15.893	14.217	1.676
419	A2052 A	15 14 17.1	+07 12 15	88.05.10	06:01	1.174	29.9	A	15.203	13.483	1.720
420	A2052 B	15 14 18.4	+07 11 14	88.05.10	06:09	1.153	29.9	A	15.790	14.145	1.645
421	A2052 C	15 14 26.4	+07 07 19	91.05.16	08:48	1.231	29.9	A	15.621	13.870	1.752
422	A2052 D	15 13 42.3	+07 08 52	91.05.16	09:05	1.289	29.9	A	16.482	14.950	1.532
427	A2063 B	15 20 45.1	+08 48 40	88.05.10	06:51	1.102	29.9	A	16.137	14.487	1.650
429	A2063 D	15 20 49.1	+08 45 02	91.07.11	06:16	1.436	29.9	A	16.051	14.440	1.611
431	A2063 F	15 20 44.5	+08 40 56	91.07.11	06:31	1.524	29.9	A	16.168	14.625	1.543
432	A2063 G	15 21 10.1	+09 31 21	91.05.18	06:42	1.086	29.9	A	15.315	13.687	1.628
436	A2107 A	15 37 27.2	+21 56 36	90.06.19	05:50	1.029	29.9	B	15.289	13.486	1.803
436	A2107 A	15 37 27.2	+21 56 36	91.05.18	06:03	1.059	29.9	A	15.221	13.448	1.772
436	A2107 A	15 37 27.2	+21 56 36	88.05.10	07:06	1.029	39.5	A	14.986	13.222	1.764
436	A2107 A	15 37 27.2	+21 56 36	90.06.19	05:59	1.034	39.5	B	15.009	13.219	1.789
438	A2107 C	15 35 14.1	+21 54 24	88.05.10	07:16	1.022	29.9	A	15.827	14.387	1.441
438	A2107 C	15 35 14.1	+21 54 24	90.06.19	06:17	1.061	29.9	B	15.874	14.350	1.524
439	A2107 D	15 37 45.0	+21 59 05	91.07.10	06:14	1.213	29.9	A	16.236	14.465	1.770
440	A2107 E	15 38 05.6	+22 04 31	91.07.10	06:33	1.283	29.9	A	16.761	15.215	1.545
443	J17 A	15 53 18.9	+41 43 24	90.08.21	04:03	1.203	29.9	A	15.089	13.444	1.644
443	J17 A	15 53 18.9	+41 43 24	88.05.08	08:30	1.017	39.5	B	14.908	13.239	1.669
443	J17 A	15 53 18.9	+41 43 24	88.05.09	08:07	1.014	39.5	A	14.927	13.244	1.683
444	J17 B	15 53 30.9	+41 43 36	90.08.21	04:10	1.237	29.9	A	16.383	14.826	1.557
446	J17 D	15 51 45.7	+41 43 37	90.08.21	04:28	1.292	29.9	A	15.364	13.744	1.620
446	J17 D	15 51 45.7	+41 43 37	88.05.08	08:37	1.019	39.5	B	15.302	13.568	1.734
446	J17 D	15 51 45.7	+41 43 37	88.05.09	08:13	1.015	39.5	A	15.233	13.583	1.650
447	J17 E	15 53 44.1	+41 42 10	91.05.18	06:57	1.021	29.9	A	16.390	14.773	1.617
453	A2147 A	16 00 00.0	+16 06 44	88.05.10	08:01	1.041	39.5	A	15.037	13.384	1.654
454	A2147 B	15 59 55.7	+16 02 43	90.06.20	05:40	1.041	29.9	B	15.483	13.758	1.725
454	A2147 B	15 59 55.7	+16 02 43	88.05.10	07:53	1.043	39.5	A	15.223	13.581	1.642
455	A2147 C	16 00 03.2	+16 29 01	88.05.10	08:11	1.038	39.5	A	14.913	13.240	1.674
456	A2147 D	16 00 01.4	+16 30 13	88.05.10	08:19	1.040	29.9	A	15.869	14.214	1.655
457	A2147 E	16 00 58.2	+16 32 22	91.05.18	07:14	1.043	29.9	A	15.707	14.006	1.701
459	A2147 G	15 58 59.4	+15 47 02	88.05.10	08:47	1.056	29.9	A	15.605	13.955	1.650
460	A2147 H	15 59 13.0	+15 38 32	88.05.10	08:32	1.048	29.9	A	15.605	13.943	1.663
461	A2147 I	16 01 27.1	+16 27 49	91.07.10	07:18	1.425	29.9	A	15.994	14.259	1.734
468	P386-1 A	15 54 58.2	+22 32 51	90.08.22	03:49	1.227	29.9	A	14.540	12.892	1.648
469	P386-1 B	15 56 07.8	+22 49 00	90.08.22	04:01	1.271	29.9	A	16.104	14.440	1.665
472	P386-2 A	16 09 15.3	+24 05 35	90.08.22	03:37	1.146	29.9	A	15.329	13.577	1.752
478	A2148 A	16 01 13.9	+25 35 25	91.07.10	07:35	1.421	29.9	A	16.892	14.928	1.964
487	J18 A	16 02 49.0	+24 04 03	91.05.17	07:51	1.010	29.9	A	15.057	13.257	1.800
488	J18 B	16 03 09.8	+23 53 25	91.05.17	08:03	1.013	29.9	A	16.070	14.441	1.629
490	J18 D	16 01 34.3	+24 13 52	91.07.11	06:47	1.244	29.9	A	16.366	14.675	1.690
495	A2151 A	16 02 20.8	+17 51 24	90.06.19	07:22	1.135	19.2	B	15.913	14.181	1.732
495	A2151 A	16 02 20.8	+17 51 24	90.06.19	07:33	1.158	29.9	B	15.418	13.663	1.755
496	A2151 B	16 02 24.6	+17 50 09	90.06.19	07:10	1.111	29.9	B	15.762	14.024	1.738
497	A2151 C	16 02 46.5	+17 54 38	90.06.21	06:28	1.063	29.9	B	15.739	14.087	1.652
498	A2151 D	16 02 54.0	+17 51 52	90.06.21	06:40	1.077	19.2	B	15.821	14.153	1.668
499	A2151 E	16 02 44.9	+18 00 18	90.06.21	07:02	1.109	19.2	B	15.861	14.266	1.595
500	A2151 F	16 03 29.7	+17 51 03	91.07.10	07:53	1.598	29.9	A	15.139	13.403	1.736
501	A2151 G	16 04 17.3	+17 50 49	90.08.23	04:14	1.345	29.9	A	16.104	14.164	1.940

Table 2 – *continued*

ID#	Name	R.A. (1950)	Dec.	Date	UT	Air	D (″)	Q	B	R	B–R
502	A2151 H	16 04 24.5	+17 53 39	90.08.23	04:30	1.408	29.9	A	15.629	13.883	1.746
505	A2151 K	16 03 25.2	+18 17 54	91.05.16	09:48	1.159	29.9	A	16.005	14.315	1.690
507	A2151 M	16 04 01.7	+18 23 00	91.05.16	10:05	1.201	29.9	A	15.259	13.539	1.720
508	A2151 N	16 03 52.2	+18 44 26	91.07.12	05:01	1.055	29.9	B	15.887	14.151	1.735
509	A2151 O	16 04 56.0	+18 46 25	91.05.16	10:21	1.248	29.9	A	15.988	14.191	1.797
511	J19 A	16 04 08.3	+15 49 08	91.05.17	08:40	1.065	29.9	A	15.430	13.707	1.723
512	J19 B	16 04 08.6	+15 49 37	91.05.17	08:50	1.080	29.9	A	15.766	14.004	1.762
513	J19 C	16 03 30.0	+15 55 30	90.06.21	05:22	1.041	39.5	B	15.424	13.765	1.659
515	J19 E	16 05 02.6	+15 58 55	91.05.15	08:45	1.064	29.9	A	16.559	14.996	1.563
516	J19 F	16 02 58.1	+16 03 37	90.06.21	05:33	1.041	19.2	B	16.626	14.849	1.777
517	J19 G	16 04 03.2	+16 33 53	90.06.21	06:12	1.056	19.2	B	16.134	14.492	1.642
518	J19 H	16 03 12.8	+16 34 12	91.05.15	08:24	1.047	29.9	A	15.610	13.865	1.745
519	J19 I	16 03 10.0	+16 34 40	91.05.15	08:05	1.039	29.9	A	16.051	14.271	1.781
522	J19 L	16 02 33.6	+16 43 09	91.05.17	09:07	1.099	29.9	A	15.842	14.141	1.701
524	J19 N	16 03 59.7	+16 10 21	91.05.17	09:23	1.128	29.9	A	16.392	14.756	1.636
528	P445-1 A	15 56 05.7	+18 13 21	91.07.12	05:22	1.094	29.9	B	15.860	14.111	1.748
529	P445-1 B	15 56 17.2	+18 00 47	91.07.12	05:59	1.167	29.9	B	16.391	14.611	1.780
530	P445-1 C	15 52 09.8	+18 47 52	91.07.12	06:15	1.209	29.9	B	15.443	13.708	1.734
533	P445-1 F	15 51 35.2	+18 29 16	91.07.12	06:26	1.254	29.9	B	16.238	14.523	1.715
534	P445-1 G	15 51 16.1	+18 30 17	91.07.12	06:41	1.313	29.9	B	16.274	14.652	1.622
536	P445-2 A	15 55 32.8	+16 27 09	90.06.21	07:14	1.153	29.9	B	15.125	13.386	1.739
536	P445-2 A	15 55 32.8	+16 27 09	90.06.21	07:19	1.164	39.5	B	14.911	13.198	1.713
538	P445-2 C	15 55 13.5	+16 05 56	90.06.21	07:31	1.197	39.5	B	14.486	12.882	1.604
539	P445-2 D	15 54 06.9	+16 40 02	90.06.21	07:37	1.213	29.9	B	15.024	13.469	1.556
540	A2162-N A	16 11 16.7	+31 01 43	90.06.20	07:10	1.064	29.9	B	16.094	14.404	1.690
540	A2162-N A	16 11 16.7	+31 01 43	90.08.21	04:42	1.298	29.9	A	16.054	14.375	1.679
543	A2162-N D	16 11 10.8	+30 57 11	90.08.21	04:57	1.359	29.9	A	15.744	14.049	1.696
546	A2162-S A	16 10 35.6	+29 36 41	90.06.20	07:02	1.049	29.9	B	14.899	13.199	1.700
546	A2162-S A	16 10 35.6	+29 36 41	88.05.10	09:31	1.037	39.5	A	14.702	13.030	1.672
547	A2162-S B	16 09 59.3	+29 58 05	88.05.10	09:44	1.053	29.9	A	15.259	13.477	1.781
548	A2162-S C	16 09 55.7	+29 57 25	88.05.10	09:52	1.067	19.2	A	16.790	15.062	1.727
551	A2162-S F	16 09 56.5	+29 34 54	91.05.15	10:07	1.131	29.9	A	16.330	14.710	1.620
552	A2162-S G	16 10 39.1	+29 46 12	91.05.15	10:26	1.175	29.9	A	15.673	13.942	1.732
553	A2162-S H	16 09 29.4	+29 34 41	91.05.15	10:43	1.222	29.9	A	16.514	14.956	1.559
554	A2162-S I	16 09 01.9	+29 39 10	91.05.15	09:48	1.095	29.9	A	16.448	14.714	1.733
557	J20 A	16 16 09.3	+35 13 51	90.06.20	06:03	1.004	29.9	B	15.396	13.771	1.624
558	J20 B	16 15 49.0	+35 07 30	90.06.20	06:16	1.007	29.9	B	15.210	13.560	1.650
559	J20 C	16 15 28.4	+35 01 23	90.06.20	06:23	1.011	29.9	B	14.941	13.240	1.701
560	J20 D	16 15 17.6	+35 00 02	90.06.20	06:29	1.015	29.9	B	15.679	14.043	1.636
562	A2197 A	16 28 04.5	+40 55 08	88.05.10	10:06	1.064	39.5	A	14.102	12.483	1.619
562	A2197 A	16 28 04.5	+40 55 08	90.06.20	07:28	1.064	39.5	B	14.092	12.471	1.621
563	A2197 B	16 26 00.7	+41 02 12	90.06.20	07:35	1.077	19.2	B	15.393	13.706	1.688
563	A2197 B	16 26 00.7	+41 02 12	88.05.10	10:20	1.085	29.9	A	14.933	13.290	1.642
564	A2197 C	16 23 29.6	+41 00 19	88.05.10	10:27	1.099	39.5	A	14.098	12.495	1.603
564	A2197 C	16 23 29.6	+41 00 19	90.06.20	07:56	1.114	39.5	B	14.104	12.483	1.621
566	A2197 E	16 28 53.1	+40 38 45	90.08.22	04:39	1.223	29.9	A	15.185	13.554	1.631
568	A2197 G	16 27 43.5	+40 58 58	91.07.10	08:05	1.356	29.9	A	15.566	14.016	1.550
571	A2197 J	16 26 58.1	+41 16 21	90.08.22	04:55	1.284	29.9	A	16.041	14.420	1.621
573	A2197 L	16 27 01.8	+41 14 45	91.07.10	08:21	1.430	29.9	A	15.597	14.038	1.559
574	A2197 M	16 29 18.7	+41 02 11	90.08.22	05:10	1.332	29.9	A	15.649	14.143	1.506
575	A2197 N	16 26 41.2	+41 00 57	90.08.23	04:46	1.277	29.9	A	16.185	14.808	1.377
580	A2199 B	16 26 40.5	+39 40 45	90.08.20	04:06	1.136	29.9	A	15.832	14.243	1.589
580	A2199 B	16 26 40.5	+39 40 45	91.07.09	06:21	1.081	29.9	A	15.848	14.238	1.610
581	A2199 C	16 26 15.9	+39 42 48	91.07.09	06:39	1.109	29.9	A	15.973	14.391	1.582
582	A2199 D	16 26 11.8	+39 22 05	91.07.09	06:56	1.142	29.9	A	15.442	13.850	1.592
583	A2199 E	16 32 06.8	+39 21 57	91.07.09	07:12	1.173	29.9	A	15.633	14.042	1.591
584	A2199 F	16 29 20.6	+39 53 54	90.08.20	04:30	1.176	29.9	A	15.017	13.414	1.604
586	A2199 H	16 29 35.9	+39 15 23	91.05.18	08:34	1.015	29.9	A	15.683	14.083	1.600

Table 2 – *continued*

ID#	Name	R.A. (1950)	Dec.	Date	UT	Air	D (″)	Q	B	R	B–R
590	A2199 L	16 25 57.7	+39 29 34	90.08.23	05:19	1.393	29.9	A	15.184	13.610	1.574
591	A2199 M	16 25 20.6	+39 38 16	90.08.23	05:07	1.343	29.9	A	15.481	13.941	1.540
593	A2199 O	16 22 33.8	+39 19 29	91.05.18	08:20	1.010	29.9	A	15.646	14.003	1.643
598	J21 A	16 36 16.1	+50 26 37	88.05.09	08:20	1.059	39.5	A	14.473	12.923	1.550
600	J21 C	16 31 55.2	+50 30 07	88.05.09	08:42	1.054	29.9	A	15.568	13.882	1.687
602	J21 E	16 31 38.6	+50 30 19	88.05.09	08:33	1.055	29.9	A	15.128	13.432	1.696
609	A2247 A	16 57 33.0	+81 42 36	91.05.17	10:02	1.566	29.9	A	15.685	13.895	1.790
610	A2247 B	16 56 56.8	+81 41 53	91.05.17	10:18	1.575	29.9	A	16.258	14.439	1.819
613	A2247 E	16 55 39.5	+81 39 16	91.05.17	10:33	1.585	29.9	A	15.970	14.185	1.786
614	A2247 F	16 53 26.9	+81 41 35	91.05.18	08:59	1.547	29.9	A	15.976	14.143	1.833
617	P332-1 A	16 59 56.2	+28 29 17	90.08.20	05:12	1.229	29.9	A	15.625	13.830	1.795
618	P332-1 B	16 59 57.3	+28 27 31	90.08.20	05:25	1.272	29.9	A	16.016	14.394	1.622
621	P332-1 E	16 58 44.3	+28 05 52	90.06.21	07:56	1.077	29.9	B	16.160	14.389	1.771
621	P332-1 E	16 58 44.3	+28 05 52	90.08.20	05:38	1.333	29.9	A	16.151	14.487	1.664
622	P332-1 F	16 57 47.2	+27 50 26	91.05.18	10:31	1.112	29.9	A	16.098	14.411	1.687
626	J22 A	16 55 58.4	+27 55 46	91.07.09	04:59	1.004	29.9	A	14.699	12.913	1.787
626	J22 A	16 55 58.4	+27 55 46	88.05.07	07:59	1.049	39.5	B	14.510	12.720	1.790
626	J22 A	16 55 58.4	+27 55 46	88.05.07	08:03	1.043	60.2	B	14.179	12.504	1.675
627	J22 B	16 54 43.4	+27 53 55	88.05.07	08:10	1.034	39.5	B	15.125	13.365	1.760
628	J22 C	16 55 29.4	+27 55 13	91.05.18	10:07	1.077	29.9	A	15.465	13.734	1.731
629	J22 D	16 56 44.4	+27 56 01	90.08.21	05:09	1.269	29.9	A	16.040	14.296	1.744
630	J22 E	16 56 51.2	+28 02 21	88.05.07	08:21	1.024	39.5	B	15.765	13.990	1.774
631	J22 F	16 55 55.3	+27 46 29	90.06.21	08:18	1.112	19.2	B	17.125	15.378	1.748
632	J22 G	16 55 42.9	+27 44 05	91.07.09	05:11	1.003	29.9	A	16.694	14.871	1.822
633	J22 H	16 55 53.6	+28 12 14	91.07.09	05:27	1.005	29.9	A	15.727	14.063	1.664
634	J23 A	17 14 31.8	+57 27 55	90.06.20	08:10	1.148	19.2	B	15.068	13.314	1.755
634	J23 A	17 14 31.8	+57 27 55	88.05.09	08:53	1.113	39.5	A	14.382	12.668	1.714
634	J23 A	17 14 31.8	+57 27 55	90.06.20	08:05	1.143	39.5	B	14.398	12.693	1.704
635	J23 B	17 14 33.0	+57 22 36	90.06.20	08:17	1.157	29.9	B	15.432	13.707	1.725
635	J23 B	17 14 33.0	+57 22 36	88.05.09	09:00	1.110	39.5	A	15.244	13.575	1.669
636	J23 C	17 13 46.0	+57 21 38	90.06.20	08:29	1.175	19.2	B	16.207	14.529	1.677
639	J24 A	17 31 31.9	+43 47 34	88.05.09	09:30	1.023	29.9	A	15.307	13.677	1.631
645	J25 A	17 55 23.6	+62 37 01	88.05.09	09:42	1.165	39.5	A	14.621	12.961	1.661
646	J25 B	17 54 25.7	+62 39 04	88.05.09	09:49	1.164	29.9	A	15.278	13.589	1.689
648	J26 A	18 01 08.3	+42 47 34	91.10.14	03:09	1.310	19.2	A	15.976	14.217	1.759
648	J26 A	18 01 08.3	+42 47 34	90.06.21	08:55	1.071	29.9	B	15.662	13.923	1.739
649	J26 B	18 00 10.8	+42 43 04	91.10.05	03:28	1.262	29.9	A	16.659	14.984	1.675
653	J27 A	18 35 09.8	+51 25 22	88.05.09	10:04	1.072	39.5	A	14.641	12.952	1.689
654	J27 B	18 34 47.7	+51 24 57	88.05.09	10:14	1.067	39.5	A	15.325	13.705	1.620
655	J27 C	18 32 54.0	+51 22 22	90.06.19	08:46	1.071	29.9	B	15.774	14.104	1.670
657	J27 E	18 35 41.5	+51 29 12	90.06.19	08:58	1.080	29.9	B	16.106	14.389	1.717
658	J38 A	21 38 18.6	−16 55 21	91.10.05	03:58	1.516	29.9	A	15.523	13.702	1.821
659	J38 B	21 38 12.3	−16 56 39	91.10.04	03:10	1.568	29.9	A	16.057	14.311	1.746
662	A2506 A	22 47 32.6	+11 26 00	90.08.20	06:22	1.199	29.9	A	14.659	12.896	1.763
663	A2506 B	22 47 25.1	+11 20 36	90.06.20	09:53	1.284	29.9	B	14.478	12.751	1.727
663	A2506 B	22 47 25.1	+11 20 36	90.08.20	06:30	1.180	29.9	A	14.462	12.732	1.729
663	A2506 B	22 47 25.1	+11 20 36	90.06.20	09:58	1.267	39.5	B	14.253	12.543	1.710
664	A2506 C	22 46 55.7	+11 19 39	90.08.20	06:38	1.152	29.9	A	16.277	14.679	1.598
665	A2506 D	22 47 06.1	+11 17 29	90.08.21	06:51	1.127	29.9	A	15.237	13.559	1.677
666	A2506 E	22 47 16.4	+11 17 15	91.07.09	08:03	1.421	29.9	A	16.403	14.681	1.723
667	A2506 F	22 47 50.0	+11 15 57	90.06.20	10:05	1.223	29.9	B	15.941	14.251	1.691
668	A2506 G	22 47 48.1	+11 22 17	90.08.21	07:03	1.110	29.9	A	15.358	13.685	1.673
669	A2506 1	22 48 58.5	+11 21 57	91.07.09	08:22	1.339	29.9	A	16.141	14.425	1.716
674	A2572 A	23 16 14.0	+18 25 28	90.08.21	08:36	1.028	29.9	A	15.633	13.917	1.716
675	A2572 B	23 16 03.7	+18 28 33	90.08.21	09:01	1.032	29.9	A	15.934	14.254	1.680
676	A2572 C	23 16 00.7	+18 24 55	91.10.10	03:14	1.181	29.9	A	15.381	13.568	1.812
677	A2572 D	23 16 43.7	+18 38 15	91.10.10	03:26	1.141	29.9	A	16.496	14.714	1.782
681	A2589 A	23 21 27.0	+16 30 08	91.10.14	03:46	1.100	19.2	A	15.799	14.018	1.780

Table 2 – *continued*

ID#	Name	R.A. (1950)	Dec.	Date	UT	Air	D (″)	Q	B	R	B–R
681	A2589 A	23 21 27.0	+16 30 08	90.08.20	07:32	1.087	29.9	A	15.418	13.637	1.781
682	A2589 B	23 21 28.7	+16 32 11	90.08.22	05:57	1.296	29.9	A	16.281	14.607	1.674
683	A2589 C	23 21 17.7	+16 29 38	90.08.22	06:15	1.227	29.9	A	16.631	14.965	1.666
684	A2589 D	23 21 23.9	+16 24 21	90.08.20	07:51	1.063	29.9	A	16.663	15.009	1.655
687	A2589 G	23 21 17.2	+16 34 39	91.10.04	03:45	1.186	29.9	A	17.087	15.131	1.956
691	A2593-N A	23 21 49.2	+14 22 20	91.07.10	09:21	1.206	29.9	A	15.511	13.740	1.770
692	A2593-N B	23 21 41.3	+14 20 38	91.10.10	04:26	1.081	29.9	A	16.192	14.532	1.660
693	A2593-N C	23 22 01.2	+14 21 51	90.08.20	08:51	1.048	29.9	A	16.458	14.752	1.705
694	A2593-N D	23 22 06.3	+14 22 02	90.08.22	07:14	1.113	29.9	A	16.072	14.376	1.696
695	A2593-N E	23 22 10.3	+14 21 29	91.07.10	09:40	1.161	29.9	A	15.508	13.791	1.717
696	A2593-N F	23 21 52.1	+14 23 01	91.10.04	05:44	1.049	29.9	A	16.508	14.814	1.694
697	A2593-N G	23 22 08.8	+14 23 32	91.10.04	04:29	1.111	29.9	A	16.155	14.967	1.188
698	A2593-N H	23 22 04.9	+14 24 28	91.10.04	04:56	1.076	29.9	A	16.595	14.868	1.727
699	A2593-N I	23 21 52.7	+14 25 55	90.08.22	06:56	1.145	29.9	A	16.348	14.635	1.713
700	A2593-N J	23 21 41.1	+14 08 56	90.08.20	09:10	1.054	29.9	A	16.326	14.612	1.714
702	A2593-N L	23 23 06.6	+14 17 55	90.08.22	06:36	1.196	29.9	A	16.351	14.548	1.803
703	A2593-N M	23 22 53.8	+14 28 53	91.10.13	04:33	1.064	19.2	A	16.547	14.847	1.701
704	A2593-N 1	23 22 05.9	+14 18 31	91.10.05	04:46	1.086	29.9	A	16.728	15.115	1.612
706	A2593-N 3	23 21 30.5	+14 12 24	91.10.05	05:07	1.066	29.9	A	17.445	15.692	1.753
707	A2593-N 4	23 21 02.6	+14 18 07	91.10.13	04:51	1.053	19.2	A	17.177	15.637	1.540
709	A2593-S A	23 21 55.0	+13 41 49	90.08.20	09:27	1.064	29.9	A	15.204	13.461	1.743
711	A2593-S C	23 21 45.6	+13 41 30	91.10.04	06:10	1.054	29.9	A	16.461	14.763	1.698
712	A2593-S D	23 22 00.8	+13 59 49	91.07.09	08:55	1.309	29.9	A	16.327	14.625	1.702
713	A2593-S E	23 20 55.7	+13 51 24	91.10.13	04:16	1.081	29.9	A	16.023	14.492	1.531
715	A2593-S G	23 21 24.4	+13 38 08	91.07.09	09:49	1.147	29.9	A	17.222	15.551	1.671
717	A2634 B	23 36 08.5	+26 44 02	90.08.22	08:03	1.024	29.9	A	15.833	14.080	1.753
718	A2634 C	23 35 58.9	+26 42 05	90.08.21	10:22	1.059	29.9	A	15.735	14.012	1.723
719	A2634 D	23 35 56.5	+26 42 28	91.07.09	10:13	1.071	29.9	A	15.832	14.095	1.738
720	A2634 E	23 36 20.4	+26 59 24	90.08.21	11:06	1.130	29.9	A	15.329	13.502	1.827
721	A2634 F	23 35 27.6	+26 59 14	91.10.14	03:27	1.113	19.2	A	16.342	14.556	1.785
722	A2634 G	23 37 30.3	+26 51 21	90.08.21	09:35	1.012	29.9	A	14.823	12.940	1.883
722	A2634 G	23 37 30.3	+26 51 21	91.10.14	05:26	1.004	29.9	A	14.824	12.917	1.908
723	A2634 H	23 38 16.2	+26 33 26	90.08.21	10:54	1.103	29.9	A	15.312	13.641	1.671
724	A2634 I	23 37 19.0	+27 05 54	90.08.22	08:15	1.015	29.9	A	15.873	14.077	1.795
725	A2634 J	23 37 48.6	+27 17 02	90.08.21	10:40	1.079	29.9	A	15.476	13.699	1.776
726	A2634 K	23 38 23.7	+27 13 54	90.08.22	08:31	1.008	29.9	A	15.813	14.078	1.734
727	A2634 1	23 35 52.5	+26 52 51	91.10.14	05:10	1.005	19.2	A	16.096	14.365	1.730
728	A2634 2	23 35 48.2	+26 36 34	91.10.14	04:54	1.011	19.2	A	16.187	14.448	1.738
730	A2657 B	23 42 10.9	+08 56 16	90.08.23	08:45	1.086	29.9	A	16.836	14.850	1.986
731	A2657 C	23 41 57.5	+08 59 09	91.10.14	07:20	1.206	29.9	A	16.087	14.214	1.873
733	A2657 E	23 41 51.7	+08 53 12	90.08.23	07:20	1.176	29.9	A	16.367	14.519	1.847
734	A2657 F	23 41 43.2	+08 46 15	90.08.22	08:46	1.088	29.9	A	16.281	14.408	1.873
735	A2657 G	23 42 28.7	+08 46 00	90.08.23	08:31	1.093	19.2	A	17.376	15.594	1.782
736	A2657 H	23 42 44.3	+08 59 37	90.08.23	07:38	1.144	29.9	A	16.505	14.641	1.864

Table 2 – *continued*

ID#	Name	R.A. (1950)	Dec.	Date	UT	Air	D (″)	Q	B	R	B–R
738	A2666 A	23 48 26.5	+26 52 07	90.08.23	06:35	1.189	19.2	A	14.821	13.107	1.714
740	A2666 C	23 48 29.1	+26 58 45	90.08.23	06:46	1.153	19.2	A	16.490	14.823	1.667
741	A2666 D	23 48 28.7	+27 00 38	90.08.23	07:03	1.115	19.2	A	16.505	15.049	1.455
765	N4874	12 57 10.0	+28 13 48	88.05.10	04:06	1.030	29.9	A	14.478	12.825	1.653
769	N4889	12 57 43.0	+28 14 42	88.05.10	04:14	1.024	29.9	A	13.927	12.272	1.655
773	N3379	10 45 11.0	+12 50 48	88.05.08	03:57	1.085	29.9	B	11.829	10.242	1.587
773	N3379	10 45 11.0	+12 50 48	88.05.09	04:25	1.127	29.9	A	11.851	10.264	1.587
773	N3379	10 45 11.0	+12 50 48	88.05.10	03:52	1.088	29.9	A	11.859	10.260	1.598
773	N3379	10 45 11.0	+12 50 48	91.05.16	05:19	1.347	29.9	A	11.863	10.264	1.599
773	N3379	10 45 11.0	+12 50 48	91.05.17	04:26	1.187	29.9	A	11.854	10.244	1.609
773	N3379	10 45 11.0	+12 50 48	88.05.08	04:00	1.088	60.2	B	11.298	9.717	1.581
773	N3379	10 45 11.0	+12 50 48	88.05.09	04:30	1.135	60.2	A	11.342	9.762	1.580
773	N3379	10 45 11.0	+12 50 48	88.05.10	03:57	1.093	60.2	A	11.359	9.777	1.582
774	N0936	02 25 04.8	−01 22 42	90.08.23	11:20	1.200	29.9	A	12.662	11.070	1.592
794	N0584	01 28 50.4	−07 07 42	90.08.22	10:32	1.288	29.9	A	12.563	10.980	1.584
794	N0584	01 28 50.4	−07 07 42	91.10.10	08:18	1.307	29.9	A	12.561	10.977	1.584
795	N0596	01 30 21.6	−07 17 18	90.08.20	10:04	1.330	29.9	A	13.019	11.489	1.530
795	N0596	01 30 21.6	−07 17 18	91.10.14	05:38	1.448	29.9	A	13.013	11.497	1.515
797	N5846	15 03 56.4	+01 47 48	88.05.07	08:36	1.212	29.9	B	13.006	11.340	1.666
797	N5846	15 03 56.4	+01 47 48	88.05.08	08:47	1.243	29.9	B	13.036	11.335	1.701
797	N5846	15 03 56.4	+01 47 48	90.06.19	04:59	1.163	29.9	B	13.105	11.390	1.716
797	N5846	15 03 56.4	+01 47 48	90.06.20	05:07	1.169	29.9	B	13.098	11.403	1.695
797	N5846	15 03 56.4	+01 47 48	90.06.21	05:11	1.175	29.9	B	13.087	11.396	1.691
797	N5846	15 03 56.4	+01 47 48	91.07.10	05:26	1.371	29.9	A	13.010	11.333	1.678
797	N5846	15 03 56.4	+01 47 48	91.07.11	04:35	1.234	29.9	A	13.017	11.326	1.691
797	N5846	15 03 56.4	+01 47 48	91.07.12	04:45	1.265	29.9	B	13.051	11.362	1.689
797	N5846	15 03 56.4	+01 47 48	90.06.19	05:03	1.165	39.5	B	12.817	11.129	1.688
797	N5846	15 03 56.4	+01 47 48	90.06.20	05:11	1.172	39.5	B	12.786	11.099	1.686
797	N5846	15 03 56.4	+01 47 48	90.06.21	05:15	1.179	39.5	B	12.772	11.096	1.675
799	N7626	23 18 10.2	+07 56 36	90.08.20	07:25	1.163	29.9	A	13.627	11.921	1.705
799	N7626	23 18 10.2	+07 56 36	90.08.22	09:03	1.098	29.9	A	13.640	11.937	1.702
799	N7626	23 18 10.2	+07 56 36	91.07.09	08:42	1.444	29.9	A	13.660	11.937	1.724
799	N7626	23 18 10.2	+07 56 36	91.07.10	10:46	1.110	29.9	A	13.624	11.921	1.703
799	N7626	23 18 10.2	+07 56 36	91.10.04	06:46	1.116	29.9	A	13.621	11.937	1.684
799	N7626	23 18 10.2	+07 56 36	91.10.05	04:33	1.156	29.9	A	13.636	11.919	1.718
799	N7626	23 18 10.2	+07 56 36	91.10.10	03:48	1.192	29.9	A	13.633	11.931	1.703
799	N7626	23 18 10.2	+07 56 36	91.10.14	04:03	1.139	29.9	A	13.648	11.937	1.711
800	N4486	12 28 17.4	+12 40 06	88.05.07	05:40	1.083	29.9	B	12.058	10.432	1.625
800	N4486	12 28 17.4	+12 40 06	91.05.16	05:25	1.102	29.9	A	12.080	10.441	1.639
800	N4486	12 28 17.4	+12 40 06	91.05.17	04:34	1.064	29.9	A	12.092	10.438	1.654
800	N4486	12 28 17.4	+12 40 06	88.05.07	05:43	1.085	60.2	B	11.284	9.669	1.615
800	N4486	12 28 17.4	+12 40 06	88.05.10	04:22	1.063	60.2	A	11.312	9.699	1.612
801	N0224	00 40 00.0	+40 59 42	91.10.05	07:30	1.015	29.9	A	10.261	8.571	1.690

Table 3. *BVR* photoelectric data.

ID#	Name	Date	UT	Air	D (″)	Q	B	V	R	B−V	B−R
209	P597-1 A	91.10.12	11:08	1.186	29.9	A	14.560	13.446	12.793	1.114	1.767
580	A2199 B	90.08.20	04:06	1.136	29.9	A	15.838	14.844	14.258	0.994	1.580
773	N3379	88.05.09	04:25	1.127	29.9	A	11.828	10.849	10.244	0.979	1.584
773	N3379	88.05.10	03:52	1.088	29.9	A	11.837	10.851	10.245	0.986	1.592
773	N3379	91.05.16	05:19	1.347	29.9	A	11.857	10.866	10.274	0.991	1.583
773	N3379	91.05.17	04:26	1.187	29.9	A	11.848	10.848	10.258	1.000	1.590
773	N3379	88.05.09	04:30	1.135	60.2	A	11.327	10.354	9.750	0.973	1.577
773	N3379	88.05.10	03:57	1.093	60.2	A	11.337	10.362	9.761	0.975	1.576
774	N936	90.08.23	11:20	1.200	29.9	A	12.661	11.685	11.087	0.976	1.574
794	N584	90.08.22	10:32	1.288	29.9	A	12.558	11.577	10.995	0.981	1.563
794	N584	91.10.10	08:18	1.307	29.9	A	12.554	11.574	10.990	0.981	1.565
795	N596	90.08.20	10:04	1.330	29.9	A	13.016	12.066	11.498	0.950	1.518
795	N596	91.10.14	05:38	1.448	29.9	A	13.008	12.076	11.509	0.932	1.498
797	N5846	90.06.19	04:59	1.163	29.9	B	13.093	12.043	11.403	1.051	1.690
797	N5846	90.06.20	05:07	1.169	29.9	B	13.085	12.038	11.401	1.047	1.685
797	N5846	90.06.21	05:11	1.175	29.9	B	13.077	12.023	11.391	1.054	1.686
797	N5846	91.07.10	05:26	1.371	29.9	A	13.008	11.963	11.340	1.045	1.668
797	N5846	91.07.11	04:35	1.234	29.9	A	13.011	11.969	11.338	1.042	1.674
797	N5846	91.07.12	04:45	1.265	29.9	B	13.043	11.994	11.368	1.049	1.675
797	N5846	90.06.19	05:03	1.165	39.5	B	12.807	11.759	11.139	1.048	1.668
797	N5846	90.06.20	05:11	1.172	39.5	B	12.774	11.727	11.096	1.047	1.677
797	N5846	90.06.21	05:15	1.179	39.5	B	12.762	11.715	11.091	1.047	1.671
799	N7626	90.08.20	07:25	1.163	29.9	A	13.625	12.561	11.930	1.063	1.694
799	N7626	90.08.22	09:03	1.098	29.9	A	13.642	12.579	11.951	1.063	1.691
799	N7626	91.07.09	08:42	1.444	29.9	A	13.654	12.582	11.948	1.072	1.706
799	N7626	91.07.10	10:46	1.110	29.9	A	13.611	12.554	11.926	1.057	1.685
799	N7626	91.10.04	06:46	1.116	29.9	A	13.616	12.564	11.950	1.052	1.666
799	N7626	91.10.05	04:33	1.156	29.9	A	13.625	12.570	11.933	1.056	1.692
799	N7626	91.10.10	03:48	1.192	29.9	A	13.626	12.570	11.943	1.056	1.683
799	N7626	91.10.14	04:03	1.139	29.9	A	13.642	12.586	11.954	1.056	1.688
800	N4486	91.05.16	05:25	1.102	29.9	A	12.075	11.059	10.453	1.016	1.622
800	N4486	91.05.17	04:34	1.064	29.9	A	12.086	11.068	10.455	1.018	1.631
801	N224	91.10.05	07:30	1.015	29.9	A	10.250	9.204	8.579	1.046	1.671

in these comparisons are observations of both standard galaxies and programme galaxies. In the results given below, each observation is counted as a separate measurement.

An intercomparison of the 98 duplicate observations taken on quality A or B nights yields 1σ errors per observation of 0.027 mag in B, 0.023 mag in R and 0.018 mag in $B-R$ colour. In comparison, errors from photon statistics alone are 0.007, 0.006 and 0.009 mag respectively. While the scatter in the galaxy magnitudes is dominated by effects other than photon noise, the scatter in the colours is only twice as great as the photon noise. This suggests that the scatter in the repeat measurements is dominated by the photometric stability of the night, consistent with our estimates of 1–3 per cent stability from the standard star observations.

In contrast, the 96 comparisons of nights of quality C both with themselves and with better quality nights yield much larger 1σ errors of 0.063 mag in B, 0.042 mag in R and 0.034 mg in $B-R$. All of these errors are large compared to the photon statistics. Inspection of the individual comparisons reveals that most of the difference between the quality C nights and the better nights comes in the form of a number of large deviations, often 0.15–0.30 mag in both B and R. Even when the magnitude deviation is large, however, the amplitude is similar in both passbands, so that the colour is little affected. This implies that extinction variations are the cause of the large scatter in the magnitudes from the quality C nights.

2.2.2 *BVR versus BR photoelectric reductions*

For the galaxies with *BR* photometry alone, R magnitudes were obtained from the standard stars using only the B and R magnitudes. For those galaxies with *BVR* photometry, R magnitudes were obtained using both the *BR* reduction and a separately determined *BVR* reduction. The 33 *BVR* galaxy observations are given in Table 3, and can be compared with *BR* reductions for the same observations in Table 2. Unfortunately, on the nights of 1988 May 7 and 8, the only nights observed with Cold Box # 27 which were of quality A or B, standard galaxies were not observed in the V filter. The observations of NGC 4486 on the night of 1988 May 10 also did not include the V filter.

The data for all standard stars were reduced using both a *BR* reduction and a *BVR* reduction. The reduction procedures ensured that there were no systematic differences between the two reduction schemes for the magnitudes and the colours of the standard stars.

The result for the 10 galaxies with *BVR* photometry is somewhat different. In Fig. 1 we plot for the 33 observations of these galaxies the difference in B, R and $B-R$ magnitudes (in the sense of *BR* reduction minus *BVR* reduction) as a function of $B-R$ colour from the *BR* reduction. The data are separated into two groups according to photomultiplier and filter set used: four observations made with the GaAs system (circles) and 29 observations made with the S-20 system (squares). The GaAs observations were made during

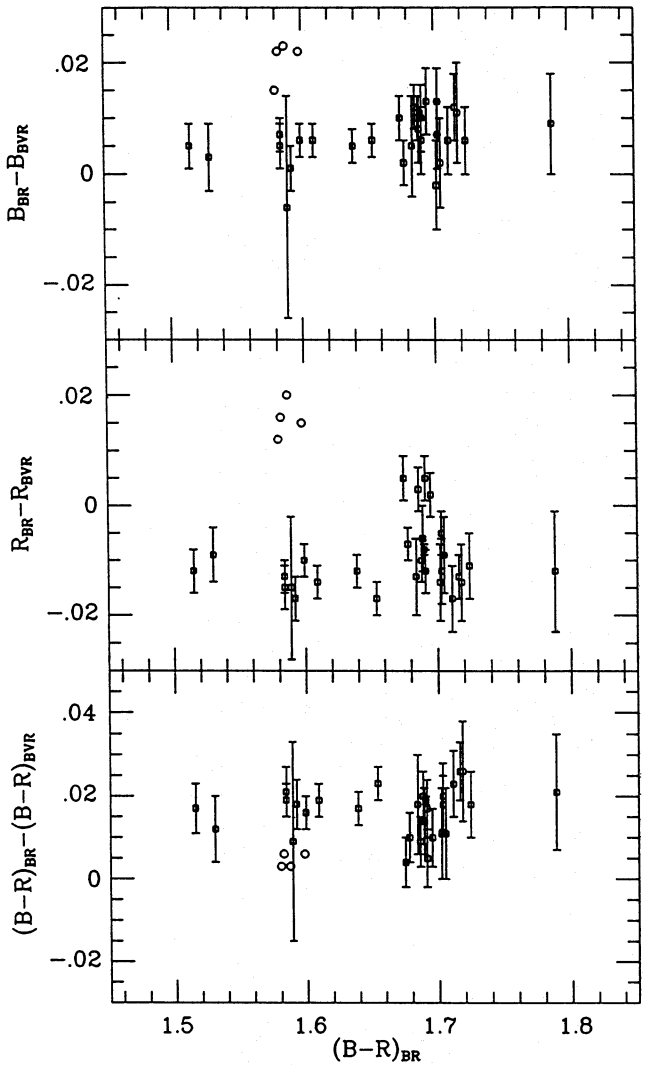

Figure 1. Comparison of *BR* and *BVR* reductions of photoelectric observations of galaxies (circles = GaAs, squares = S-20).

one run of two nights, while the S-20 data were obtained over many runs and many nights. The *BR* reduction for the S-20 system predicts galaxy B magnitudes that are 0.007 mag too faint relative to the *BVR* reductions, R magnitudes that are -0.012 mag too bright, and $B-R$ colours that are 0.02 mag too red. The same comparisons for the GaAs observations yield *BR*-predicted B magnitudes that are 0.02 mag fainter than the *BVR* B magnitudes, R magnitudes that are 0.018 mag fainter, and $B-R$ colours that are 0.005 mag redder.

These systematic differences cannot be due to differences in extinction, as they are consistent for all nights observed, and are not seen for the standard stars. Rather, we believe that these kinds of systematic difference arise from the fact that galaxy spectral energy distributions are not those of stars. The 800-Å widths of the *BVR* passbands apparently allow 1–2 per cent differences in the transformation coefficients between galaxies and stars to occur.

All of the programme galaxy CCD data have been obtained using a *BR* system. Hence it was decided to publish the photoelectric observations from the *BR* reduction to minimize systematic differences between the photoelectric and CCD data sets. As will be shown later in this paper, the systematic difference in R magnitude between the GaAs system and the S-20 system is of similar size to the errors that exist between the CCD and photoelectric data.

2.3 External comparisons

Of all the photoelectric data given in this paper, very little can be compared in a straightforward manner to published data. Few R-passband data exist on galaxies, especially on the Landolt photometric system. An accurate external check on the reliability of the photoelectric (or CCD) magnitude requires either a precisely matched aperture or the use of a luminosity profile or growth curve for each galaxy. The latter type of comparison will be deferred to a future paper, in which we will present all of our CCD data.

Only the $B-V$ colours of those galaxies with measured *BVR* magnitudes are suitable for external comparison in this paper. *BVR* photometry is available, of course, for the standard galaxies. In addition, one programme galaxy, P597-1 A (NGC 1713), was observed in *BVR* and has published *BV* data. The $B-V$ comparisons are summarized in Table 4. Sources of external photometry are given in the notes to Table 4, and are the same as were used in the analysis of Burstein et al. (1987). The number code for each source is the same as given in table 4 of Burstein et al., and the transformations of the *BV* observations of each source to a 'standard' *BV* system are those used in that paper.

A total of 11 separate aperture observations of nine galaxies can have the new measurements of $B-V$ colour made here compared to existing measurements in the literature. The criterion for comparison is the same as used in Burstein et al., namely that the difference in aperture size between our data and a literature source cannot be greater than 0.05 dex. Most galaxies in this comparison have multiple observations in our survey, and multiple comparisons to literature data. Of the 45 aperture measurements taken from the literature, 24 come directly from the Burstein et al. survey while 21 come from other sources. The mean of the zero-point differences between our new measurements and those from the literature is only -0.007 ± 0.005 mag. The standard deviation of the differences about this value is 0.016 mag. It should also be noted that the galaxy with only one published colour and one observation by us (P597-1 A) also has the largest difference in $B-V$ colour, which is consistent with the dispersion observed between single observations by two different observers in Burstein et al. (1987).

The accuracy implied for the individual measurements is 0.011 mag, within a factor of 2 of the accuracy obtained for the best standard star observations. The fact that no significant $B-V$ zero-point offset is found in our data relative to the literature can be principally attributed to the fact that the *BVR* reduction package used here was also used for the data given in Burstein et al. (1987).

To summarize the results of this section, we find by internal comparisons that the B and R photoelectric magnitudes for our galaxies should be accurate to 2–3 per cent, while the $B-R$ colours should be accurate to 1–2 per cent. An external check of $B-V$ colours indicates that these colours are of 1 per cent accuracy when multiply observed.

Table 4. External comparisons of photoelectric photometry.

Name	N_{obs}	log A	ΔB−V	$B-V_{new}$	$\langle B-V_{cat}\rangle$	$B-V_{cat}$	Source
N224	1	0.70	0.001	1.046	1.045	1.04	1
						1.05	20
N584	2	0.70	-0.001	0.980	0.981	0.98	1
						0.98	4
						0.99	5*
						0.97	15
						0.985	20
						0.98	22
						0.98	25
N596	2	0.70	-0.026	0.941	0.967	0.97	1
						0.98	5*
						0.98	15
						0.98	20
						0.95	20
						0.94	23
N936	1	0.70	-0.028	0.976	1.004	1.005	1
						1.000	5*
						1.03	1
						0.98	20
N3379	4	0.70	-0.012	0.988	1.000	1.02	1
						0.99	3
						0.99	21
						1.00	37
N3379	2	1.00	-0.002	0.977	0.979	0.975	1
						0.966	5*
						0.97	7
						1.00	15
						0.97	32
						0.99	37
N4486	2	0.70	0.010	1.017	1.007	1.046	2*
						0.99	3
						0.99	5*
						1.00	21
						1.01	26
N5846	6	0.70	0.008	1.048	1.040	0.99	5*
						1.06	21
						1.07	37
N5846	3	1.00	0.016	1.051	1.035	1.035	2*
						1.04	7
						1.02	15
						1.04	21
						1.04	37
N7626	7	0.70	-0.011	1.059	1.070	1.05	15
						1.07	20
						1.09	22
						1.06	23
P597-1 A	1	0.70	-0.031	1.114	1.145	1.145	27†

Sources: (1) de Vaucouleurs & de Vaucouleurs (1972); (2) Tifft (1961, 1963, 1969, 1973); (3) de Vaucouleurs et al. (1978); (4) Persson, Frogel & Aaronson (1979); (5) Sandage & Visvanathan (1978); (7) Sandage (1972, 1973, 1975); (15, 20–27, 37) Burstein et al. (1987); (32) Kormendy (1977). *Transformed following Burstein et al. (1987). †N1713, average of 0.51 and 0.81 log *A* apertures.

3 CCD PHOTOMETRY

3.1 Observations

The photometric CCD data for this paper were obtained during two observing runs on the 1.0-m Jacobus Kapteyn Telescope (JKT) at La Palma over the nights of 1990 October 15–17 and 1991 May 9–13. The detectors were two similar GEC CCDs (GEC3 in 1990, GEC6 in 1991), both with a pixel size of 0.30 arcsec, a field of 2.9×1.9 arcmin^2 and a gain of 1.0 e^- adu^{-1}. As spatial resolution was not critical, the CCDs were binned 2×2 on-chip to reduce readout noise. Mould *B* and *R* filters (Argyle et al. 1988) were used for both runs.

Since the aim of this project was to obtain photometry for the programme galaxies accurate to better than 3 per cent, care was taken with both the observing strategy and the reduction procedure. However, there is clearly a trade-off between the amount of observing time spent on standard stars and that spent on the objects of interest. The following observing strategy was therefore adopted to ensure enough calibration data to parametrize the photometric conditions sufficiently, whilst leaving most of the observing time free for our programme galaxies.

Bias frames were taken in the usual way at the beginning and end of each night. Sky flats were also taken each night during evening and morning twilight, as these were found to be superior to dome flats which leave residual structure after flat-fielding. Standard stars, selected from Landolt's (1983) tables of *UBVRI* standards, were observed in *B* and *R* throughout each night. These stars were usually observed out of focus in order to maximize the signal whilst remaining in the linear regime of the CCD's response. A minimum of four or five standard stars were observed at least twice in both *B* and *R* at the beginning of the night. These were selected to give a good sky coverage at a range of airmasses and a broad span of $B-R$ colours. Using software available at the telescopes, instrumental magnitudes were computed as the observations were taken. Standard stars were repeatedly observed until we were confident that the atmosphere was stable and photometric across the whole sky.

Consistent with our experience with the photoelectric data, analysis of various CCD runs gave a rule of thumb that fluctuations of more than 0.03 mag in repeat observations of standard stars indicated that conditions were insufficiently photometric. Groups of standard stars would be observed every 60 to 80 min during the night. These groups would typically consist of three stars observed twice in *B* and *R*, again selected to give good sky and colour coverage. Five or more standard stars would be observed in the same way at the end of the night. For an observation of a programme galaxy to be declared photometric, it had to be bracketed by two sets of standard star measurements, each with rms errors of less than 0.03 mag.

Table 5 is a log of the observations for each of the nine photometric nights, giving the telescope and CCD together with the photometric periods of the night. The table also lists the number of standard star observations, the number of different standard stars observed, the rms residual of these observations about the fitted photometric transformation (see below) and the number of galaxies imaged in photometric conditions. Exposure times for galaxies ranged from 150 to 600 s. The galaxies were generally only observed in the *R* filter, although some previously well-studied galaxies were also observed in *B* in order to permit comparisons with earlier work.

3.2 Data reductions

All CCD images of both standard stars and galaxies underwent the same basic reduction procedure. The images were first bias-subtracted, using the median of the 10 or so bias images taken before and after each night's run scaled to the mean level of the CCD's overscan strip. No correction for dark current was made, as this was negligible on both CCDs. Tests of the CCD response curves showed no evidence for non-linearity over the relevant range of counts. Flat-field corrections were made by dividing each image by the median

Table 5. Log of CCD observations.

Date	Telescope	CCD	Photometric period (UT)	# std obsns	# std stars	*rms* residual (mag)	# gal obsns
90.10.15	JKT 1m	GEC3	0105–0631	38	9	0.017	12
90.10.16	"	binned 2x2	1952–0259	65	13	0.027	17
90.10.17	"	"	2049–0523	36	7	0.026	9
91.05.09	JKT 1m	GEC6	2347–0521	61	12	0.020	7
91.05.10	"	binned 2x2	2054–0528	57	13	0.010	18
91.05.11	"	"	2037–0351	46	12	0.009	6
91.05.13	"	"	2047–0535	77	17	0.007	28
			Total:	380	83		97

of the twilight sky images taken in the appropriate filter. The resulting images had residual flat-field variations of less than 1 per cent rms.

Instrumental magnitudes for the standard stars were determined using either the FIGARO FOTO routine or the IRAF QPHOT task. In both cases the magnitudes were measured within synthetic apertures much larger than the stars' images, which were usually taken deliberately out of focus in order to obtain as high a signal as possible without saturating the CCD. The sky level about each standard star was estimated as the mode of the pixel values in an annulus at large radius about the star. The results of these measurements were in excellent agreement with the instrumental magnitudes obtained using the PHOT on-line software during the observations.

In order to reduce the instrumental magnitudes to the standard *BR* photometric system, we parametrized the photometric transformations as

$$M_{BR} = M_{\rm obs} - \alpha \times \text{airmass} - \beta \times (B-R) - \gamma - \delta_i,$$

where $M_{\rm obs}$ is the observed stellar magnitude, α is the coefficient of extinction, β is the colour correction, γ is an overall zero-point, and the δ_i are zero-point corrections determined at various times during the night. The δ_i terms are simply additive corrections to the fit for each group of standard star observations, and so provide a means of tracking temporal changes in atmospheric conditions. A linear interpolation between the two δ_i terms bracketing a given galaxy observation is used in computing a photometric zero-point for that observation. This procedure allows changing atmospheric conditions to be modelled as well as the standard star data permit, but care must be taken that there are enough standard stars to ensure that the δ_i terms represent real changes in the extinction.

The parameters of the photometric transformation were determined using an iterative multilinear regression technique. This procedure was as follows. (i) Solve for α, β and γ using multilinear regression. (ii) The δ_i term for each group of standard stars is then simply the mean difference between the measured magnitudes for each group and this solution. On the second and subsequent iterations the δ_i terms from the previous iteration are included in the fit. (iii) The fit is subtracted from the data and the process is repeated either until further iterations do not improve the rms residual by more than some small amount (here 0.001 mag), or until a maximum of 100 iterations is reached. Graphical checks of the solutions were made to avoid bias from 'wild' observations. We have tested this procedure with simulated data and established that it leads to accurate and reliable solutions. Our photometric data typically required 8–12 iterations to converge to a solution.

The method we use to determine a galaxy's integrated magnitude from a CCD image is quite different from the direct measurement of the light in circular apertures employed by photoelectric photometry. Although this latter approach could be mimicked by using synthetic apertures, the real aim of the CCD photometry is to determine the galaxy's surface brightness profile accurately, uncontaminated by superimposed stars or galaxies. Before determining magnitudes, we therefore delete contaminating objects by setting all the pixels in regions fully covering their images to a 'magic' value, indicating that the flux in these pixels is undetermined. A comparison of the CCD magnitudes with and without deletions is made in Section 4. The sky level is estimated as the mode of the pixel values in selected areas on the CCD frame, excluding the deleted regions and the area covered by the target galaxy. Given that almost all the galaxies are small compared to the size of the CCD frame (with the exception of #773=NGC 3379), this method gives robust and precise estimates of sky – for the 1990 October run the mean estimated error in the sky level was 0.8 per cent, while for the 1991 May run it was 1.0 per cent. The centre of the galaxy's image is then established by centroiding over a small region about the peak of the light. The circularized surface brightness profile about this centre is computed as the azimuthal average of the flux in radial steps of one pixel. The flux at any given radius and azimuth is estimated by bilinear interpolation using the four nearest pixels. If the flux in any of these four pixels is undetermined (i.e. the pixel is set to the 'magic' value), then the flux being estimated is also considered to be undetermined. At a radius of N pixels, the azimuthally averaged flux is computed as the mean over approximately $2\pi N$ points uniformly distributed in azimuth (so the sampled points are approximately one pixel apart). Points at which the flux is undetermined are omitted when calculating the mean. The resulting circularized surface brightness profile is converted to instrumental magnitudes and then integrated out to the appropriate radius (using linear interpolation) in order to compare the CCD magnitude to the photoelectric magnitude within the corresponding aperture.

Instrumental CCD magnitudes determined in this way were transformed on to the standard system using the extinction coefficient, colour term and overall zero-point for the night. A zero-point correction was also applied, as interpolated from the corrections derived for the two groups of stars bracketing the galaxy observation. Since only an R image was obtained for the galaxies, we assumed a $B-R$ colour of 1.7

in every case. As the photoelectric data show, this is the mean colour for these E and S0 galaxies. The bluest galaxy in the sample has $B-R=1.37$, while the reddest has $B-R=1.96$; the standard deviation about the mean colour is 0.11 mag. The mean absolute value of the colour terms we obtain is 0.010; the maximum is 0.021. Thus the typical error we make by assuming all our sample have $B-R=1.7$ is 0.001 mag, and the maximum possible error for a single galaxy is 0.007 mag.

4 COMPARISON OF PHOTOELECTRIC AND CCD PHOTOMETRY

There are 95 programme galaxies for which we can compare photoelectric and CCD photometry. Table 6 summarizes this comparison. The name, date, time and airmass of the CCD observation are given, together with the diameter (in arcsec) of the photometric aperture. This diameter is chosen to match the aperture used in the photoelectric observations of the galaxy. There are 97 comparisons listed in Table 6: NGC 3379 (# 773) was observed with two different photoelectric apertures and separate CCD magnitudes were computed for each; J11 E (# 306) has two photometric CCD observations, so differences from the photoelectric magnitude are given for both. For galaxies with more than one photoelectric observation at the same aperture, the observations were averaged before being compared to the CCD magnitude. Table 6 lists the mean R_{PE} and $(B-R)_{PE}$, the difference $\Delta R = R_{CCD} - R_{PE}$ for each comparison and the quality of the nights on which the photoelectric and CCD data were taken (indicated by class A or B for the photoelectric data and by the rms residual of the calibration for the CCD data).

The distribution of these differences is shown in Fig. 2. The mean difference between the CCD and photoelectric magnitudes for all 97 comparisons is $\overline{\Delta R} = -0.004$ mag and the standard deviation about the mean is $\sigma_{\Delta R} = 0.036$ mag. Although the distribution appears double-peaked, a battery of tests for deviations from a Gaussian distribution (part of the ROSTAT software: Beers, Flynn & Gebhardt 1990) shows no inconsistency with a single Gaussian distribution at even the 10 per cent confidence level. Since the rms errors in the photoelectric magnitudes estimated from repeat observations are 0.02–0.03 mag (Section 2.2.1), the scatter of 0.036 mag in ΔR implies that the rms precision of the CCD magnitudes is also 0.02–0.03 mag.

For the 38 comparisons using data from the 1990 October CCD run, we find $\overline{\Delta R} = -0.010$ mag and $\sigma_{\Delta R} = 0.030$; for the 59 comparisons using the 1991 May CCD data, $\overline{\Delta R} = 0.000$ mag and $\sigma_{\Delta R} = 0.039$. The mean ΔR values for these two runs differ by only 1.4 times their joint standard error. Fig. 3 shows how ΔR varied with time during each night of CCD observations. Rank correlation tests (Spearman's ρ and Kendall's τ) show no evidence for any night having a significant trend of ΔR with time. Two nights, both with fewer than 10 comparisons, show small but statistically significant overall offsets: 1990 October 17 has $\overline{\Delta R} = -0.022$ mag (2.8 times the standard error in the mean) and 1991 May 9 has $\overline{\Delta R} = +0.031$ mag (2.6 times the standard error in the mean). The scatter ΔR on all nights was in the range $\sigma_{\Delta R} = 0.02$–0.04 mag.

Both quality A and quality B photoelectric observations are consistent with zero offset between the two photometric systems. For the 90 comparisons using photoelectric data of quality A, $\overline{\Delta R} = -0.004$ mag and $\sigma_{\Delta R} = 0.036$ mag, while for the seven quality B comparisons $\overline{\Delta R} = -0.010$ mag and $\sigma_{\Delta R} = 0.043$ mag.

Fig. 4(a) shows that the fainter ($14 < R < 15$) galaxies in the sample have a scatter $\sigma_{\Delta R} = 0.038$ mag, close to the value for the sample as a whole, while the brighter ($R < 14$) galaxies show significantly less scatter: $\sigma_{\Delta R} = 0.026$ mag. The increase in the scatter with R magnitude is consistent with the estimated error of ~ 1 per cent in the sky level, since in the 19.2- and 29.9-arcsec apertures the sky flux becomes comparable to that from the galaxy at around $R = 14$. By $R = 15$ the error in sky contributes a couple of per cent to the overall magnitude error, resulting in the observed increase in the scatter. There is no trend of $\overline{\Delta R}$ with R magnitude.

Neither the mean nor the scatter of the differences varies with the galaxy's $B-R$ colour (Fig. 4b), the airmass of the CCD observation (Fig. 4c) or the aperture size used to make the measurement (Fig. 4d). The relatively large difference found for the one comparison at an aperture diameter of 60.2 arcsec (# 773 = NGC 3379, $\Delta R = +0.065$ mag) is probably due to the fact that this large galaxy nearly fills the

Table 6. CCD photometry and comparison with photoelectric photometry.

ID#	CCD Image	Date	UT	Air	D (")	R_{CCD}	R_{PE}	$(B-R)_{PE}$	R_{CCD}-R_{PE}	Q	*rms*
1	A76_A_582	90.10.16	00:38	1.09	29.9	13.375	13.379	1.846	−0.004	A	0.027
2	A76_B_583	90.10.16	00:40	1.09	29.9	14.171	14.206	1.695	−0.035	A	0.027
4	A76_D_585	90.10.16	00:48	1.09	29.9	14.034	14.023	1.755	+0.011	A	0.027
96	A260_A_350	90.10.15	01:55	1.01	29.9	13.322	13.340	1.776	−0.018	A	0.017
98	A260_C_351	90.10.15	02:03	1.01	29.9	13.723	13.712	1.760	+0.011	A	0.017
100	A260_E_353	90.10.15	02:17	1.02	29.9	14.012	14.020	1.735	−0.008	A	0.017
101	A260_F_354	90.10.15	02:24	1.03	29.9	13.924	13.935	1.735	−0.011	A	0.017
102	A260_G_355	90.10.15	02:30	1.03	19.2	14.292	14.273	1.762	+0.019	A	0.017
122	J8_A_601	90.10.16	01:54	1.00	29.9	13.778	13.741	1.803	+0.037	A	0.027
127	J8_F_604	90.10.16	02:08	1.01	29.9	14.177	14.184	1.903	−0.007	A	0.027
128	J8_G_605	90.10.16	02:12	1.01	19.2	14.225	14.240	1.826	−0.015	A	0.027
130	J8_I_607	90.10.16	02:21	1.01	19.2	14.665	14.690	1.937	−0.025	A	0.027
137	A376_C_728	90.10.17	02:24	1.01	29.9	14.886	14.904	1.759	−0.018	A	0.026
151	A397_A_733	90.10.17	02:47	1.03	19.2	14.403	14.414	1.859	−0.011	A	0.026
153	A397_C_734	90.10.17	02:51	1.03	19.2	14.444	14.467	1.808	−0.023	A	0.026
154	A397_D_735	90.10.17	02:55	1.04	19.2	14.639	14.705	1.831	−0.066	A	0.026
155	A397_E_734	90.10.17	02:51	1.03	29.9	14.816	14.793	1.782	+0.023	A	0.026
158	A397_H_732	90.10.17	02:43	1.03	19.2	14.915	14.942	1.909	−0.027	A	0.026
160	A400_A_367	90.10.15	03:16	1.10	29.9	13.775	13.798	1.869	−0.023	A	0.017
163	A400_D_368	90.10.15	03:22	1.11	29.9	14.370	14.374	1.900	−0.004	A	0.017

Table 6 – *continued*

ID#	CCD Image	Date	UT	Air	D (″)	R_{CCD}	R_{PE}	$(B-R)_{PE}$	R_{CCD}-R_{PE}	Q	*rms*
164	A400_E_369	90.10.15	03:30	1.12	29.9	13.885	13.866	1.858	+0.019	A	0.017
166	A400_G_371	90.10.15	03:42	1.14	29.9	14.655	14.637	1.746	+0.018	A	0.017
200	J34_E_746	90.10.17	03:26	1.43	19.2	14.573	14.591	1.732	−0.018	A	0.026
201	J34_F_747	90.10.17	03:38	1.42	29.9	13.591	13.607	1.752	−0.016	A	0.026
209	P597-1_A_383	90.10.15	04:51	1.15	29.9	12.799	12.781	1.788	+0.018	A	0.017
210	P597-1_B_384	90.10.15	05:00	1.16	29.9	13.555	13.560	1.758	−0.005	A	0.017
211	P597-1_C_385	90.10.15	05:09	1.16	19.2	13.909	13.858	1.774	+0.051	A	0.017
273	A548-1_H_751	90.10.17	03:56	1.84	29.9	13.618	13.659	1.616	−0.041	A	0.026
302	J11_A_765	91.05.13	23:12	1.10	29.9	13.875	13.870	1.602	+0.005	A	0.007
306	J11_E_043	91.05.09	00:41	1.16	29.9	14.235	14.177	1.370	+0.058	A	0.020
306	J11_E_767	91.05.13	23:20	1.11	29.9	14.197	14.177	1.370	+0.020	A	0.007
307	J11_F_768	91.05.13	23:24	1.11	39.5	13.906	13.899	1.571	+0.007	A	0.007
321	J13_D_237	91.05.10	22:08	1.09	29.9	13.853	13.866	1.772	−0.013	A	0.010
333	J13_P_238	91.05.10	22:13	1.00	29.9	14.464	14.465	1.625	−0.001	A	0.010
387	J16_E_443	91.05.11	22:22	1.47	29.9	14.100	14.112	1.676	−0.012	A	0.009
388	J16_F_444	91.05.11	22:25	1.46	19.2	14.701	14.754	1.716	−0.053	A	0.009
399	J16-W_E_072	91.05.11	23:45	1.17	29.9	14.186	14.172	1.615	+0.014	B	0.009
406	A2063-S_A_258	91.05.10	23:34	1.18	29.9	13.472	13.507	1.685	−0.035	A	0.010
408	A2063-S_C_259	91.05.10	23:40	1.17	29.9	14.416	14.374	1.741	+0.042	A	0.010
427	A2063_B_278	91.05.10	00:47	1.08	29.9	14.499	14.487	1.650	+0.012	A	0.010
429	A2063_D_280	91.05.10	00:58	1.07	29.9	14.357	14.440	1.611	−0.083	A	0.010
431	A2063_F_279	91.05.10	00:53	1.07	29.9	14.581	14.625	1.543	−0.044	A	0.010
432	A2063_G_281	91.05.10	00:03	1.06	29.9	13.661	13.687	1.628	−0.026	A	0.010
439	A2107_D_282	91.05.10	01:18	1.01	29.9	14.455	14.465	1.771	−0.010	A	0.010
440	A2107_E_283	91.05.10	01:13	1.01	29.9	15.119	15.215	1.546	−0.096	A	0.010
447	J17_E_483	91.05.11	01:03	1.04	29.9	14.799	14.773	1.617	+0.026	A	0.009
453	A2147_A_815	91.05.13	02:54	1.06	39.5	13.402	13.384	1.653	+0.018	A	0.007
455	A2147_C_817	91.05.13	03:03	1.07	39.5	13.214	13.240	1.673	−0.026	A	0.007
456	A2147_D_817	91.05.13	03:03	1.07	29.9	14.233	14.214	1.655	+0.019	A	0.007
457	A2147_E_486	91.05.11	01:19	1.04	29.9	14.029	14.006	1.701	+0.023	A	0.009
459	A2147_G_818	91.05.13	03:09	1.09	29.9	13.939	13.955	1.650	−0.016	A	0.007
460	A2147_H_819	91.05.13	03:13	1.09	29.9	13.967	13.943	1.662	+0.024	A	0.007
461	A2147_I_487	91.05.11	01:24	1.03	29.9	14.243	14.259	1.734	−0.016	A	0.009
478	A2148_A_304	91.05.10	02:24	1.01	29.9	14.935	14.928	1.964	+0.007	A	0.010
487	J18_A_300	91.05.10	02:07	1.00	29.9	13.237	13.257	1.800	−0.020	A	0.010
488	J18_B_301	91.05.10	02:11	1.00	29.9	14.419	14.441	1.629	−0.022	A	0.010
507	A2151_M_307	91.05.10	02:36	1.03	29.9	13.545	13.539	1.720	+0.006	A	0.010
508	A2151_N_308	91.05.10	02:39	1.03	29.9	14.162	14.151	1.736	+0.011	B	0.010
509	A2151_O_309	91.05.10	02:43	1.03	29.9	14.209	14.191	1.797	+0.018	A	0.010
511	J19_A_064	91.05.09	03:57	1.14	29.9	13.693	13.707	1.723	−0.014	A	0.020
512	J19_B_064	91.05.09	03:57	1.14	29.9	14.031	14.004	1.762	+0.027	A	0.020
518	J19_H_065	91.05.09	04:02	1.15	29.9	13.900	13.865	1.745	+0.035	A	0.020
519	J19_I_065	91.05.09	04:02	1.15	29.9	14.335	14.271	1.780	+0.064	A	0.020
522	J19_L_079	91.05.09	04:33	1.24	29.9	14.195	14.141	1.701	+0.054	A	0.020
524	J19_N_081	91.05.09	04:43	1.27	29.9	14.752	14.756	1.636	−0.004	A	0.020
528	P445-1_A_310	91.05.10	02:48	1.04	29.9	14.031	14.111	1.749	−0.080	B	0.010
529	P445-1_B_311	91.05.10	02:52	1.04	29.9	14.668	14.611	1.780	+0.057	B	0.010
558	J20_B_837	91.05.13	04:13	1.13	29.9	13.542	13.560	1.650	−0.018	B	0.007
559	J20_C_838	91.05.13	04:18	1.15	29.9	13.223	13.240	1.701	−0.017	B	0.007
560	J20_D_838	91.05.13	04:18	1.15	29.9	14.009	14.043	1.636	−0.034	B	0.007
574	A2197_M_839	91.05.13	04:23	1.14	29.9	14.094	14.143	1.506	−0.049	A	0.007
575	A2197_N_840	91.05.13	04:27	1.15	29.9	14.777	14.808	1.377	−0.031	A	0.007
581	A2199_C_841	91.05.13	04:31	1.16	29.9	14.361	14.391	1.582	−0.030	A	0.007
582	A2199_D_842	91.05.13	04:36	1.17	29.9	13.896	13.850	1.592	+0.046	A	0.007
586	A2199_H_777	91.05.13	00:18	1.12	29.9	14.058	14.083	1.600	−0.025	A	0.007
590	A2199_L_843	91.05.13	04:40	1.18	29.9	13.577	13.610	1.574	−0.033	A	0.007
591	A2199_M_844	91.05.13	04:44	1.19	29.9	13.933	13.941	1.540	−0.008	A	0.007
593	A2199_O_778	91.05.13	00:23	1.10	29.9	13.983	14.003	1.643	−0.020	A	0.007
609	A2247_A_821	91.05.13	03:23	1.66	29.9	13.917	13.895	1.790	+0.022	A	0.007
610	A2247_B_821	91.05.13	03:23	1.66	29.9	14.503	14.439	1.819	+0.064	A	0.007
613	A2247_E_822	91.05.13	03:29	1.66	29.9	14.209	14.185	1.785	+0.024	A	0.007
614	A2247_F_823	91.05.13	03:34	1.66	29.9	14.174	14.143	1.833	+0.031	A	0.007
622	P332-1_F_845	91.05.13	04:49	1.12	29.9	14.363	14.411	1.687	−0.048	A	0.007
632	J22_G_847	91.05.13	04:58	1.15	29.9	14.972	14.871	1.823	+0.101	A	0.007
633	J22_H_848	91.05.13	05:02	1.16	29.9	14.032	14.063	1.664	−0.031	A	0.007
677	A2572_D_521	90.10.16	20:59	1.12	29.9	14.729	14.714	1.782	+0.015	A	0.027
703	A2593-N_M_528	90.10.16	21:29	1.10	19.2	14.846	14.847	1.700	−0.001	A	0.027
704	A2593-N_1_529	90.10.16	21:33	1.09	29.9	15.038	15.115	1.613	−0.077	A	0.027
711	A2593-S_C_543	90.10.16	22:17	1.05	29.9	14.667	14.763	1.698	−0.096	A	0.027
712	A2593-S_D_544	90.10.16	22:21	1.04	29.9	14.602	14.625	1.702	−0.023	A	0.027
713	A2593-S_E_545	90.10.16	22:25	1.04	29.9	14.451	14.492	1.531	−0.041	A	0.027
715	A2593-S_G_547	90.10.16	22:34	1.04	29.9	15.592	15.551	1.671	+0.041	A	0.027
721	A2634_F_548	90.10.16	22:38	1.01	19.2	14.528	14.556	1.786	−0.028	A	0.027
731	A2657_C_565	90.10.16	23:27	1.06	29.9	14.220	14.214	1.873	+0.006	A	0.027
738	A2666_A_567	90.10.16	23:42	1.00	19.2	13.085	13.107	1.714	−0.023	A	0.027
773	N3379_733	91.05.13	21:41	1.08	60.2	9.834	9.769	1.582	+0.065	A	0.007
773	N3379_733	91.05.13	21:41	1.08	29.9	10.264	10.258	1.599	+0.006	A	0.007

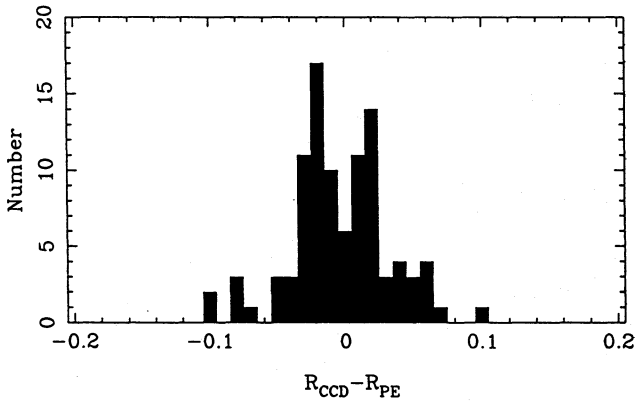

Figure 2. The distribution of the difference between CCD and photoelectric R magnitudes for 97 comparisons at various apertures of 95 galaxies.

CCD frame. The estimate of the sky level may therefore be biased upwards, leading to over-subtraction of sky and an overly faint CCD magnitude, especially in larger apertures (in the 29.9-arcsec aperture this galaxy has $\Delta R = +0.006$).

We have checked the effect on the photoelectric magnitudes of contaminating sources within the photometric apertures by also deriving CCD magnitudes *without* deleting nearby objects. We find that only nine of the galaxies in Table 6 have their R_{CCD} changed by more than 0.02 mag. When the CCD magnitude *without* deletions is used in the comparison with the photoelectric magnitudes, only six of these nine actually show a smaller ΔR and the overall scatter is not improved. Examination of the CCD images shows that not deleting other objects makes little difference to the comparison simply because the original apertures used in the photoelectric photometry were well chosen to avoid bright contaminating sources.

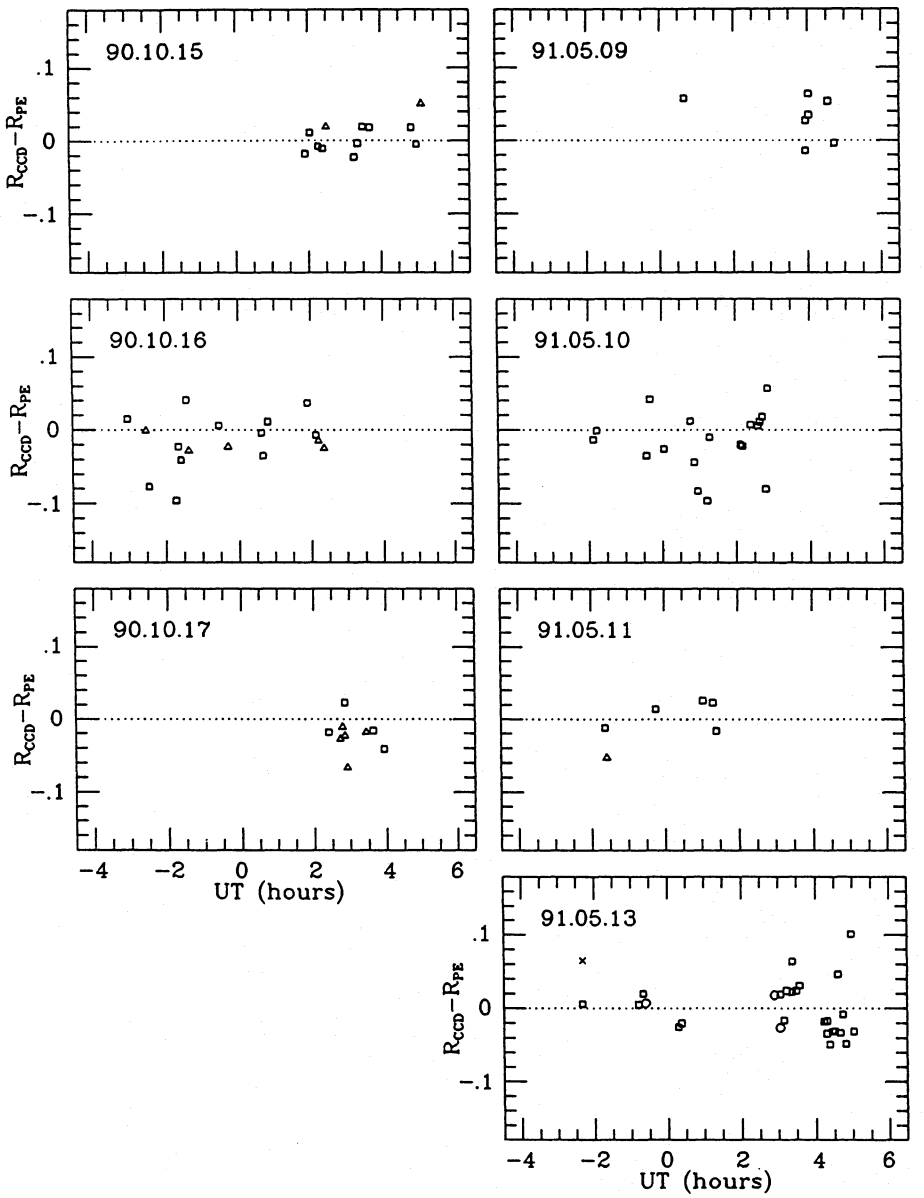

Figure 3. The temporal variation in R_{CCD} on each of the nights with CCD photometry, as shown by the differences $R_{CCD} - R_{PE}$. The different symbols indicate aperture sizes: triangles = 19.2 arcsec; squares = 29.9 arcsec; circles = 39.5 arcsec, and crosses = 60.2 arcsec.

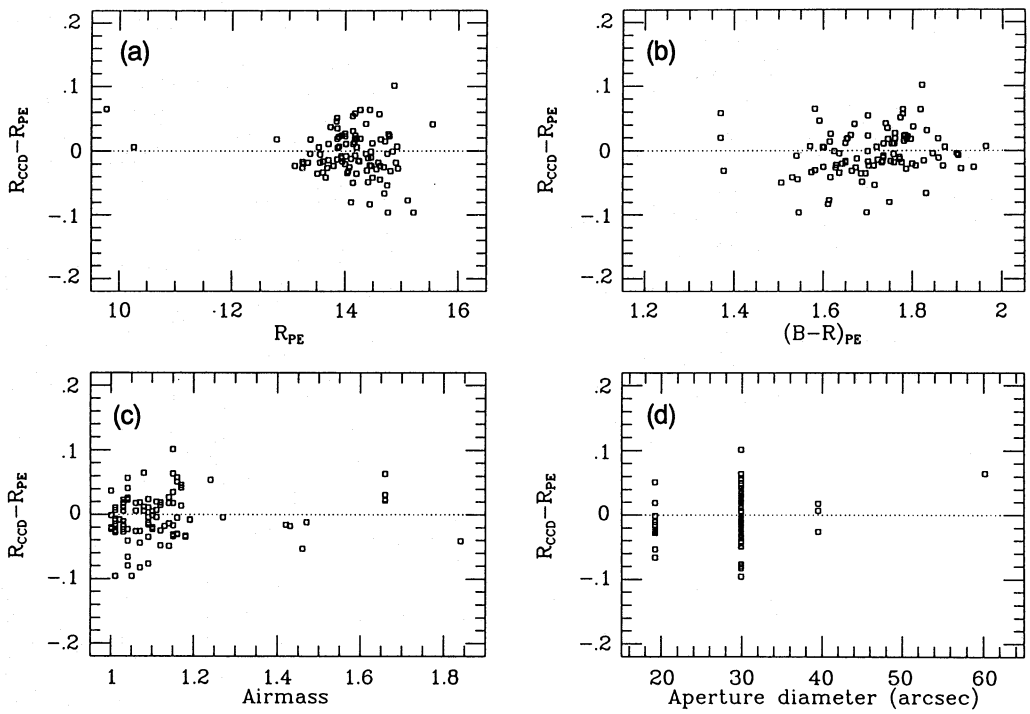

Figure 4. The distribution of differences $R_{CCD}-R_{PE}$ with (a) photoelectric magnitude R_{PE}, (b) $(B-R)_{PE}$ colour, (c) the airmass of the CCD observation, and (d) the aperture diameter (in arcsec) used when measuring the magnitudes.

5 CONCLUSIONS

In this paper we have presented *BR* photoelectric photometry for 352 E and S0 galaxies and *BVR* photoelectric photometry for 10 galaxies. These observations are part of a large programme to study the properties and peculiar motions of these galaxies. The aims of this paper are to show, first, that even for relatively distant, faint galaxies ($R \lesssim 15$) it is possible to obtain magnitudes with a precision of at least 3 per cent and, secondly, that a photometric system can be established for both photoelectric and CCD photometry that has a common zero-point to within 1 per cent and negligible colour terms for E and S0 galaxies.

A comparison of the 98 repeat *BR* photoelectric observations in our data set shows the rms errors on individual B and R magnitudes to be 2–3 per cent and on $B-R$ colours to be 1–2 per cent. We have compared the results obtained for the 33 *BVR* observations using both a *BVR* reduction and a *BR* reduction. We find small (0.01–0.02 mag) systematic effects that are attributable to the differences between the spectral energy distributions of stars and galaxies. We have compared the $B-V$ colours of the galaxies with *BVR* photometry to values from the literature. The mean zero-point difference is only -0.007 ± 0.005 mag. The inferred precision for the colours of individual galaxies is 0.01 mag.

We have also compared photoelectric and CCD R magnitudes (both reduced on the *BR* system) for 95 galaxies. We give a detailed description of our CCD observing strategy and our methods for reduction of the CCD data and derivation of aperture magnitudes free from contaminating sources. We show that observation of the galaxies in the R band only and assumption of a mean $B-R$ colour introduces negligible errors in our CCD magnitudes. We find that there is excellent overall agreement (better than 1 per cent) between the zero-points of the photoelectric and CCD R magnitudes. Two of the seven nights of CCD observations, however, show zero-point differences from the photoelectric photometry of 2–3 per cent. The rms difference between the photoelectric and CCD magnitudes is 0.036 mag which, together with the estimated rms internal error of 2–3 per cent for the photoelectric photometry, implies that the rms error on individual CCD measurements is also 2–3 per cent. There is no trend in either the mean or the scatter of the differences with magnitude, colour, airmass or photometric aperture, except that brighter galaxies have slightly less scatter than the sample as a whole.

We thus have established a *BR* photometric system for photoelectric photometry which can also be applied to R-band CCD photometry of early-type galaxies, with a zero-point agreement that is good to better than 1 per cent. We have also shown that we can obtain aperture magnitudes, both photoelectrically and with CCDs, which have a precision of 2–3 per cent even for distant galaxies as faint as $R \approx 15$. Errors in galaxy magnitudes of this order introduce errors of $\lesssim 2$ per cent into D_n and the resulting distance estimates from the D_n–σ relation (Dressler et al. 1987), corresponding to errors in peculiar velocities of $\lesssim 200$ km s^{-1} for galaxies at 10000 km s^{-1}. However, photometric errors are unlikely to be the limiting factor in the precision of our D_n–σ distance estimates, since a precision of 2 per cent would be required in the measurement of velocity dispersions to achieve an equally small contribution to the errors from σ.

ACKNOWLEDGMENTS

MMC, DB, RLD and RM were Visiting Observers at Kitt Peak National Observatory, National Optical Astronomy Observatories, which is operated by the Association of Universities for Research in Astronomy, Inc., under contract

with the National Science Foundation. The Jacobus Kapteyn Telescope is operated on the island of La Palma by the Royal Greenwich Observatory in the Spanish Observatorio del Roque de los Muchachos of the Instituto de Astrofísica de Canarias. Much of the data reduction was carried out at Starlink nodes in the UK using Starlink software and the IRAF package. We thank Mike Shara, Brian McLean, James Scott and the rest of the STScI GASP team for their help in obtaining accurate positions for our galaxies. MMC acknowledges the support of a Fellowship at King's College, Cambridge. DB acknowledges the support of NSF Grant AST90-16930. GW acknowledges partial support from NSF grant AST90-17048 and from Margaret Anne & Edward Leede '49. EB acknowledges support from NSF grant AST90-01762. Support for travel and collaborative meetings was provided by NATO grant CRG900159, Dartmouth College and the University of Oxford.

REFERENCES

Argyle R. W., Mayer C. J., Pike C. D., Jorden P. R., 1988, La Palma User Manual No. XVIII, A User Guide to the JKT CCD Camera. Royal Greenwich Observatory, p. A34
Beers T. C., Flynn K., Gebhardt K., 1990, AJ, 100, 32
Burstein D., Davies R. L., Dressler A., Faber S. M., Stone R. P. S., Lynden-Bell D., Terlevich R., Wegner G., 1987, ApJS, 64, 601
de Vaucouleurs G., de Vaucouleurs A., 1972, Mem. R. Astron. Soc., 77, 1
de Vaucouleurs G., de Vaucouleurs A., Corwin H. G., 1978, Second Reference Catalogue of Bright Galaxies. Univ. Texas, Austin
Dressler A., Lynden-Bell D., Burstein D., Davies R. L., Faber S. M., Terlevich R., Wegner G., 1987, ApJ, 313, 42
Faber S. M., Wegner G., Burstein D., Davies R. L., Dressler A., Lynden-Bell D., Terlevich R. J., 1989, ApJS, 69, 763
Jørgensen I., Franx M., Kjærgaard P., 1992, A&AS, 95, 489
Kormendy J., 1977, ApJ, 214, 359
Landolt A. U., 1983, AJ, 88, 439
Persson S. E., Frogel J. A., Aaronson M., 1979, ApJS, 39, 61
Sandage A., 1972, ApJ, 176, 21
Sandage A., 1973, ApJ, 183, 711
Sandage A., 1975, ApJ, 202, 563
Sandage A., Visvanathan N., 1978, ApJ, 223, 707
Tifft W. G., 1961, AJ, 66, 390
Tifft W. G., 1963, AJ, 68, 302
Tifft W. G., 1969, AJ, 74, 354
Tifft W. G., 1973, PASP, 85, 283